FACULDADE DE ENGENHARIA DA UNIVERSIDADE DO PORTO

U. PORTO

FEUP FACULDADE DE ENGENHARIA
UNIVERSIDADE DO PORTO

Fast Assessment of Dynamic Behavior Analysis with Evaluation of Minimum Synchronous Inertia to Improve Dynamic Security in Islanded Power Systems

João Pedro da Silva Megre Barbosa

Mestrado Integrado em Engenharia Eletrotécnica e de Computadores

Supervisor: Prof. Dr. João Abel Peças Lopes

Second Supervisor: Dr. Bernardo Silva

July 26, 2019

Abstract

Wind and solar energy have largely contributed to the sustainability, external energy independence from coal, oil and gas suppliers and the de-carbonisation of the energy sector. Consequently, the European Union targets and policies on renewable-based electricity generation have been defined. During the last decades, the ambitious plans to achieve these targets led to massive investments and consequent installation of wind and solar power plants. To tackle this energy transition, even more investments and adoption of carbon-free energy sources are expected to be considered by the EU-member countries in the next decades, especially because of its technological maturity and cost declining. In islanded power systems, where conventional power production is mainly provided by thermal generators, usually characterized by high production costs that result from high fuel prices and cost of transportation, wind and solar power are an interesting economic option.

Despite its environmental and economic advantages, variable renewable energy sources like wind and solar power, carry some technical challenges that must be efficiently addressed so that its integration limitation and under exploitation could be avoided. For small-islanded power systems, disturbances such as sudden wind speed and irradiation changes may lead to large frequency deviations and rates of change of frequency if no control actions to compensate the resulting power imbalance be adopted. For this type of power systems, any disturbance that may occur is of particular concern due to the steady replacement of conventional generation by generation based on renewable sources interfaced by power electronics, resulting on a low inertia power system. Therefore, the loss of rotational inertia present in the system takes place and system's stability and robustness, when facing a disturbances, is jeopardized.

In order to achieve the envisioned wind and solar energy penetration in the generation mix of islanded power systems, it is urgent that new methodologies, to quickly and accurately predict systems dynamic behaviour and to suggest preventive control actions to the system operator, be developed. Therefore, this thesis presents an approach capable of evaluating power system stability and identifying the minimum synchronous inertia required to ensure system's dynamic security, in real-time, for a specific operation scenario and to support the decision maker to perform the activation of synchronous condensers in case of instability detection. The approach was developed based on trained artificial neural networks and by applying a sensitivity analysis, which makes possible the evaluation of the minimum synchronous inertia to ensure the system's security relative to system variables.

After performing several simulations for different operation scenarios and disturbances, the approach developed proved to be able to quickly and accurately identify the minimum synchronous inertia that must be present in the system to avoid load shedding or even system collapse, especially when the operation scenario is heavily based on wind and solar generation.

ii

Resumo

A energia eólica e solar tem contribuido largamente para a sustentabilidade, independência energética externa dos fornecedores de carvão, petróleo e gás e para a descarbonização do setor energético. Consequentemente, metas e políticas da União Europeia (UE) para geração de eletricidade com base renovável têm sido definidas. Durante as últimas décadas, os planos ambiciosos para atingir estas metas conduziram a investimentos massivos e consequente instalação de parques eólicos e solares. Para resolver esta transição energética é esperado que mais investimentos e adoção de fontes de energia livres de carbono sejam considerados pelos estados membros da UE na próxima década, devido à sua maturidade tecnológica e custo decrescente. Em sistemas isolados, onde a produção convencional é principalmente fornecida por geradores térmicos, usualmente caracterizados pelos elevados custos de produção que resultam dos elevados preços do combustível e do seu transporte, a energia eólica e solar constitui uma opção economicamente interessante.

Apesar das suas vantagens económicas e ambientais, as fontes variáveis de energia renovável, como é o caso da energia eólica e solar, acarretam alguns desafios técnicos que devem ser devidamente endereçados para que a integração deste tipo de fontes não seja restringida e a sua sub-exploração seja evitada. No caso de pequenos sistemas elétricos isolados, perturbações como a variação repentina da velocidade do vento e dos níveis de radiação solar, podem conduzir a grandes desvios de frequência e elevadas taxas de variação de frequência caso nenhuma ação de controlo, para compensar o desequilíbrio entre produção e consumo, seja adotada. Neste tipo de sistemas, qualquer perturbação que possa ocorrer é de particular interesse devido à substituição da geração convencional por geração renovável ligada à rede através de conversores eletrónicos, dotando o sistema de muito pouca inércia. Assim sendo, a perda de inércia síncrona presente no sistema ocorre e a estabilidade do sistema, bem como a sua robustez face a perturbações, é comprometida.

Para atingir a participação de energia eólica e solar prevista no sistema eletroprodutor dos sistemas isolados, é urgente que novas metodologias capazes de prever rapidamente e de forma precisa o comportamento dinâmico dos sistemas, assim como sugerir ações de controlo preventivo, sejam desenvolvidas. Posto isto, esta dissertação apresenta uma abordagem capaz de avaliar a estabilidade do sistema e identificar a inércia síncrona mínima necessária para garantir a segurança dinâmica do sistema, em tempo real, para um determinado cenário de operação, e apoiar o operador do sistema na tomada de decisão de colocar em funcionamento compensadores síncronos em caso de instabilidade. A abordagem foi desenvolvida com recurso ao uso de redes neuronais e através da aplicação de uma análise de sensibilidades que torna possível a avaliação da inércia síncrona mínima para garantir a segurança do sistema relativamente às variáveis do sistema.

Após várias simulações terem sido efetuadas para diferentes cenários de operação e diferentes contingências, a abordagem desenvolvida mostrou-se capaz de identificar de forma rápida e precisa a inércia síncrona mínima que deve estar presente no sistema para evitar o deslastre de cargas ou ainda, o colapso do próprio sistema, especialmente quando o cenário de operação é caracterizado pela elevada produção de energia eólica e solar.

Acknowledgements

This master thesis is the result of the work that I have been developing at FEUP (*Faculdade de Engenharia da Universidade do Porto*) during the last months. I am very proud to be a student in this institution, where I have the opportunity to learn with persons internationally recognized for their contributions and dedication in Electric Power Systems field.

I would like to thank my thesis supervisor, Prof. Dr. João Abel Peças Lopes, Full Professor of the Electrical and Computer Engineering Department at FEUP, for his help, constant motivation and skilled guidance over time. His enthusiasm and experience were crucial to the accomplishment of this thesis.

I also want to thank my co-supervisor, Dr. Bernardo Silva, Area Manager at INESCTEC Porto, for all the support and his valuable contribution to the work developed.

To my family, my father Óscar, my mother Ângela and my sister Inês. I would like to express my sincere gratitude for all the unfailing support they gave me throughout my whole life.

A special thanks to Jéssica for her continuous encouragement, optimism and friendship over the last years.

I am also very thankful to my friends for their friendship and all the good moments spent together.

Thank you,

João Megre Barbosa

"It always seems impossible until it's done."

Nelson Mandela

Contents

List of Figures

List of Tables

List of Abbreviations

AC	Alternating Current
AGC	Automatic Generation Control
ANN	Artificial Neural Network
APC	Active Power Control
CIG	Converter-interfaced Generation
COI	Center of Inertia
DC	Direct Current
DFIWG	Doubly Fed Induction Wind Generator
ESS	Energy Storage System
EU	European Union
FLL	Frequency Locked Loop
FSIWG	Fixed Speed Induction Wind Generator
MPP	Maximum Power Point
MPPT	Maximum Power Point Tracking
OPLL	Optimizing Phase Locked Loop
PLL	Phase Locked Loop
PMSG	Permanent Magnet Synchronous Generator
PMU	Phasor Measurement Unit
p.u.	Per Unit
PV	Photovoltaic
RES	Renewable Energy Sources
RES-E	Renewable Energy Source in Electricity
RMSE	Root Mean Square Error
RoCoF	Rate of Change of Frequency
SC	Synchronous Condensers
SCADA	Supervisory Control and Data Acquisition
SG	Synchronous Generator
STATCOM	Static Synchronous Compensator
SVC	Static Var Compensators
TSO	Transmission System Operator
UC	Unit Commitment
UFLS	Under Frequency Load Shedding
VSG	Virtual Synchronous Generator
VSWT	Variable Speed Wind Turbine
VSynC	Virtual Synchronous Controlled

Chapter 1

Introduction

In this chapter, a brief overview of the addressed problem will be presented. First, the motivation to the development of this thesis will be discussed, referring the importance and the need to develop fast approaches to deal with the prediction of systems dynamic behavior and easily determine preventive control actions to help on-line system management and operation. Then, the purpose of this thesis will be explained. Finally, the organization of this thesis will be exposed.

1.1 Motivation

Electrical power systems are moving towards large-scale integration of renewable power sources for electricity generation, especially wind and solar power production. The reasons for that approach are based on environmental and economical concerns. It is then necessary to drive the power system towards energy independence, namely from coal, oil and gas suppliers, and to reduce the greenhouse gases emissions produced by the electric power sector. In the European Union (EU) integration of renewable power production deserves serious consideration. Substantial progress has been made towards the accomplishment of the EU targets of 20% for renewable-based electricity generation, also called as Renewable Energy Source in Electricity (RES-E). However, the goal of 20% of renewable share in electricity generation, first proposed by the 2008 European Commission Climate and Energy Package, has been raised to 30% [16]. Moreover, the European Council endorsed a binding EU target of at least 40% domestic reduction in greenhouse gas emissions by 2030 compared to 1990 levels and at least 27% is set for the share of renewable energy consumed in the EU in 2030 [17].

Therefore, to achieve such ambitious targets, an increase in the adoption of carbon-free electric energy resources must be considered by the EU-member countries in the next decade. Regarding the energy framework, wind and solar power have provided a large contribution to allow a considerable increase of renewable energy share in electricity generation mix. Whenever wind and solar is available, both wind and solar power are also an interesting economic option, especially in isolated power systems. In these systems, global production costs of electricity can be reduced if wind and solar power production is increased, particularly in cases where conventional power

production is mainly provided by diesel generators, that are characterized by high production costs that result from high fuel price and cost of transportation.

However, power systems based in wind and solar production are exposed to sudden wind speed and irradiation changes leading to production changes that must be fast and efficiently compensated by conventional generators. Otherwise, large frequency deviations or even system collapse may occur. For small-islanded power systems, these disturbances are of particular concern, not only because islanded power systems are obviously not properly interconnected to other systems of bigger dimension but also because of the steady replacement of conventional generation by generation based on renewable sources interfaced by power electronics introduces a fragile operation. Such transition is leading to the loss of rotational inertia, which is the main reason for grid's stability and robustness when facing disturbances, making islanded power systems more fragile to any disturbance that could occur in the system. To avoid these dynamic problems, a very conservative policy of operation dispatch is usually adopted, leading to an increase in the spinning reserve requirements, to under exploitation of wind and solar power production and to high production costs.

Therefore, the envisioned wind and solar energy contribution can only be attained with the adoption of advanced control systems and methodologies to quickly and accurately predict the dynamic response of a power system, in real-time, so that economically efficient and dynamically safe operating strategies could be defined. Such approach will avoid the utilization of emergency measures like load shedding.

As a result, the work developed in this thesis proposes a methodology to identify the minimum synchronous inertia required to ensure the dynamic security of an islanded power system for a certain power dispatch and therefore, suggesting fast preventive control actions to the system operators to prevent system collapse.

1.2   Objectives

The successful integration of renewable energy sources (RES) in power systems, especially in islanded power systems, requires the identification and development of specific control functionalities able to predict system dynamic behavior after a disturbance occurs.

Conventional power stations like thermal and hydro power units have been responsible for keeping power systems dynamically stable by providing synchronous inertia, useful to avoid higher frequency deviation and rate of change of frequency (RoCoF) than the acceptable limits. However, due to the replacement of this type of generators by non-synchronous RES, using power electronic converters, system's dynamic security is under risk.

Therefore, the main objective of this thesis is to develop a methodology capable of identifying the minimum synchronous inertia required to ensure the dynamic security of an islanded power system, characterised by high levels of wind and solar penetration. This methodology must be able to perform a fast assessment of dynamic behavior and evaluate the minimum synchronous

inertia to improve dynamic security in the power system for a specific operation scenario. If successful, the developed methodology can be used for continuous monitoring of system security and be responsible for presenting to system operators adequate preventive control actions, namely the activation of synchronous condensers (SC) that should be installed in the system, redispatching power units or determining secure unit commitment (UC) alternatives in case of insecure scenarios.

1.3 Structure of the Thesis

This thesis is divided into six chapters and one appendix which are organized as follows:

Chapter 1 introduces the topic and presents the main objectives this work aims to achieve, as well as the motivation of this thesis.

Chapter 2 aims to present the main drivers and challenges for the deployment of RES, more specifically wind and solar energy sources, in power systems, specially in islanded power systems. This chapter is intended to range from background overview related to power systems stability and frequency control to the state-of-the-art research work performed to present what is already developed in each concept related to this thesis. The main challenges and technological limitations for RES penetration in islanded power systems are also addressed. Moreover, in this chapter, it is presented in the last section a general overview regarding SC and their impacts in the system's dynamic behavior.

In chapter 3 it is first presented the methodology adopted in order to achieve the objectives of this work, followed by the presentation of all the dynamic models developed in the simulation platform (MATLAB/SIMULINK) so that dynamic studies for the power system could be performed. This chapter also aims to present an overview and description of the power system used as case study of this work, as well as the framework adopted to create all the possible operation scenarios to be simulated in MATLAB/SIMULINK for frequency response analysis. Additionally, in this chapter, the two disturbances considered for the development of this thesis are also described.

Chapter 4 aims to present some background regarding the use of machine learning techniques, specifically artificial neural networks (ANN), for fast assessment of power systems' dynamic security, followed by the framework adopted for ANNs design purpose. Therefore, feature selection and data set generation processes are highlighted in this chapter and the performance of the ANNs is also presented. Moreover, in order to perform a fast dynamic security assessment using ANNs, it is presented a technique developed in this work which emphasizes the ANNs frequency response emulation capacity and relies on a sensitivity analysis of the output relative to the control variables.

In chapter 5, a detailed evaluation of the performance of the proposed tool for fast assessment of the dynamic security of the system through extensive numerical simulations is also presented. The chapter is divided into two major sections concerning the dynamic response in the simulation platform and the minimum synchronous inertia evaluation for both contingencies, respectively. The first section aims to present the results of the system dynamic response obtained in MATLAB/SIMULINK by using the model developed in this simulation platform for contingency 1 and

2. The second section concerns the presentation of the most relevant results of this work. It is in this section that ANNs frequency response emulation capacity is assessed as well as the capacity that the developed tool has to identify the minimum synchronous inertia required to guarantee that the power system is dynamically secure for a specific operation scenario.

Chapter 6 describes the main contributions of this work followed by general conclusions and perspectives for future work.

In Appendix A are presented the parameters of the dynamic models of thermal and hydro units used for the development of this work, as well as the complete dynamic model developed in MATLAB/SIMULINK to describe the expected dynamic frequency behavior of the power system.

Chapter 2

Backgrounds and State of the Art

2.1 Introduction

This chapter has the purpose of presenting important aspects, concepts, as well as new methodologies and future researches related to the topic of this thesis. Therefore, the structure of this chapter has three sections. The first one concerns power systems stability, where a brief explanation of the importance that swing equation of Synchronous Generators (SG) and inertia constant has to power systems frequency stability. The increasing integration of non-synchronous RES in isolated power grids, as well as the technical challenges imposed by this type of power sources and their limitations, are addressed in the second section of this chapter. Additionally, in the third section, the main features and the effect of SCs for the stability enhancement are also presented.

2.2 Power Systems Stability

Modern societies are even more dependent on electricity and, as a consequence, electrical power systems are becoming increasingly complex in order to meet all the electric needs, at least cost and meeting all the reliability, security and quality of service requirements.

During the exploitation of an electrical power system, it is necessary to ensure that production is able to continuously feed the consumption with voltage and frequency levels within the acceptable technical limits of operation [15], so that electrical devices could work properly.

One of the main aspects to consider in electrical power systems operation is the stability of synchronous machines since power systems rely on them for the generation of electrical energy [15]. It is well known that this type of machines tend to synchronously work under normal operating conditions. However, when a severe disturbance occurs, synchronous machines may lose their synchronism, leading to load shedding, cascade tripping and, in the worst case, system collapse. Therefore, stability studies are used to know the behavior of these type of machines when the system suffers a disturbance such as an instantaneous load or generation change. Moreover, with these studies, it is possible to evaluate the capacity that a system has to operate properly not only

under normal conditions, but also when a contingency occurs and all the SGs remain in synchronism. This is the so-called system robustness and, therefore, the more robust the system is, the greater is its capacity to remain stable after a disturbance.

The frequency of a power system is one of the most important references that indicate the system stability, security, quality and reliability. Frequency stability is the ability of a power system to maintain frequency within certain acceptable limits after a severe disturbance resulting from a significant imbalance between generation and consumption. Frequency stability relies on the ability to maintain or restore equilibrium between generation and load, with minimum unintentional loss of load [18]. The instability that may occur can lead to generation units and load tripping.

2.2.1   Swing Equation

Considering the important role that synchronous machines play in frequency control, in this subsection the equations of motion of a synchronous machine will be presented, which is relevant to understand how these type of machines can inherently contribute to system stability. As mentioned in the previous chapter, when an unbalance between the mechanical torque and the electromagnetic torque is verified, the net torque that will cause acceleration or deceleration is given by:

$$T_a = T_m - T_e \qquad (2.1)$$

where

T_a is the accelerating torque in Nm

T_m is the mechanical torque in Nm

T_e is the electromagnetic torque in Nm

The combination between the inertia of the generator and turbine is accelerated by the unbalance that result from the different torques applied to the rotor. Therefore, the equation of motion is

$$J\frac{d\omega_m}{dt} = T_a = T_m - T_e \qquad (2.2)$$

where

J is the combined moment of inertia of generator and turbine in $kg \cdot m^2$

ω_m is the angular velocity of the rotor in rad/s

t is the time in seconds

Moreover, the angular acceleration of the rotor can be express as follows:

$$\alpha = \frac{d\omega_m}{dt} = \frac{d^2\theta_m}{d^2t} \qquad (2.3)$$

where

α is the angular acceleration of the rotor in rad/s^2

θ_m is the angular position of the rotor in radians with respect to a fixed reference

However, it is usual to measure the angular rotor position with respect to a synchronously rotating reference. Thus,

$$\theta_m = \omega_m t + \delta_m \tag{2.4}$$

where

ω_m is the angular velocity of the machine

δ_m is the angular position of the rotor in electrical radians with respect to a synchronously rotating reference

Therefore, taking the time derivative and substituting in equation 2.2, we have

$$J\frac{d^2\delta_m}{d^2t} = T_a = T_m - T_e \tag{2.5}$$

Considering power P as the result of the multiplication between torque T and angular velocity ω, we have

$$J\omega_m\frac{d^2\delta_m}{d^2t} = P_a = P_m - P_e \tag{2.6}$$

where

P_m is the mechanical power of the turbine of the generator

P_e is the electrical power supplied by the generator

P_a is the acceleration power applied to the rotating mass

Moreover, SGs are characterized by their inertia constant H, defined as the kinetic energy stored in the rotating mass at rated speed, divided by the machine rating power as shown in 2.7.

$$H = \frac{W_k}{S_r} = \frac{J\omega_{m,0}^2}{2S_r} \tag{2.7}$$

where

W_k is the kinetic energy stored in the rotating mass at rated speed in watt-seconds

S_r is the machine rating power in Volt-ampere

$\omega_{m},0$ is the rated mechanical angular velocity in rad/s

In table 2.1, typical values of the inertia constant H for thermal and hydraulic generating units are presented. These values are in MWs per MVA rating of the machine.

Table 2.1: Typical values of *H*, [15]

Type of Generating Unit	H
Thermal Unit	
(a) 3600 r/min (2-pole)	2.5 to 6.0
(b) 1800 r/min (4-pole)	4.0 to 10.0
Hydraulic Unit	2.0 to 4.0

Additionally, because δ is expressed in radians and ω in radians per second, equation 2.8 can be expressed by substituting equation 2.7 in 2.6, as follows:

$$\frac{2H}{\omega_m}\frac{d^2\delta}{d^2t} = P_a = P_m - P_e \, (p.u.)$$ (2.8)

Considering that $\omega_m = 2\pi f$ and the damping factor D in, equation 2.8 can be rewritten, as follows:

$$\frac{2H}{2\pi f}\frac{d^2\delta}{d^2t} + D\frac{d\delta}{dt} = P_a = P_m - P_e \, (p.u.)$$ (2.9)

Equation 2.9 is the equation of motion of a synchronous machine, also called swing equation.

2.2.2   Inertia in Power Systems

In order to avoid faster frequency deviations and a less stable frequency behavior, which may causes the violation of the dynamic security restrictions, it is important that power systems have the necessary available rotational inertia. Therefore, system inertia is considered as one of the most relevant parameters upon which the synchronized operation of power systems is based since the inertia present in the rotating masses of the SGs determines the immediate frequency response to possible inequalities in the power balance [19].

According to [20], inertia is the resistance of a physical object to a change in its state of motion, including changes in its speed and direction. Therefore, in a traditional power system, the objects are the SGs and turbines as well as induction generators and motors connected to the power system. The resistance to the change in rotational speed is expressed by the moment of inertia J of the rotating mass. When a frequency change occurs, usually due generation or consumption change or due a short-circuit on the system, the rotating masses will inject or absorb kinetic energy into or from the electric grid so that frequency deviation could be counteracted [19]. Therefore, the lower the system inertia, the less robust the system is to abrupt changes in generation and consumption.

In figure 2.1, it is shown the influence of inertia constant on system frequency behavior. A reduced amount of inertia leads to a faster drop of frequency and therefore, it could lead to a violation of the minimum frequency limit, which could result in load shedding through the actuation of underfrequency relays. On the other hand, a larger amount of inertia slows down the initial frequency drop, which gives enough time for generator frequency control loops to intervene.
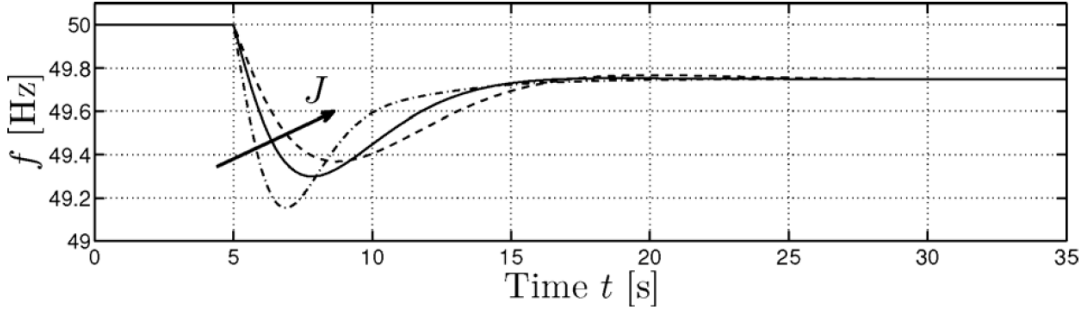
Figure 2.1: Frequency deviation for different values os system inertia constant [1]

Conventional synchronous generation units are synchronously linked to the grid so their mechanical rotational speed is directly coupled with the electrical angular frequency [19]. Thus, the motion of each generator can be expressed as in equation 2.2. The unit of H is second (s), that defines the time during which the total rotational energy stored by the masses can be used to deliver their rated power [21]. Considering a real power system with n generators connected to the grid, the overall system inertia will be the aggregation of each generator inertia constant and their rated power as well as the total rated power of the system generators, as follows:

$$H = \frac{\sum_n^{i=1} H_i S_{n,i}}{S_{system}} \tag{2.10}$$

where

H_i is the inertia constant of the i-th generator

$S_{n,i}$ is the rated power of the i-th generator

S_{system} is the total rated power of the generators in the system

Therefore, the overall inertia in a power system can be interpreted as the resistance which kinetic energy exchange from synchronous machines to counteract the changes in frequency when power imbalances between generation and demand occur [19]. Equation 2.11, which express the RoCoF after the loss of a generation unit, shows that RoCoF is dependent on the size of the unit lost and the amount of available stored kinetic energy [15, 22].

$$\frac{df}{dt} = \frac{f_0 P}{2 H_{system} S_b} \tag{2.11}$$

where

P is the size of the production lost

H_{system} is the system inertia constant

f_0 is the nominal system frequency

S_b is the rating power of the system

2.3   Frequency Control and Stability

2.3.1   Inertial Frequency Response

The inertial frequency response is intrinsic in the system due to the rotating masses of conventional generation and the typical load (pumps, motor, etc.) [23]. This frequency response constitutes the first stage of systems frequency control strategy, as described in figure 2.2, so that frequency deviation can be arrested within seconds, figure 2.3. This first stage is responsible for limiting high RoCoF in order to provide sufficient time for the activation and deployment of primary frequency control, which compose the second phase of frequency control procedure so that the trigger of RoCoF protection of SGs and their consequent cascading tripping could be avoided [24].

Figure 2.2: Frequency regulation stages [2]

Figure 2.3: Typical time scale of frequency regulation [3]

As mentioned in the previous section, the rotating masses of the generators and motors allow the storage of kinetic energy. Moreover, the amount of kinetic energy stored is proportional to the
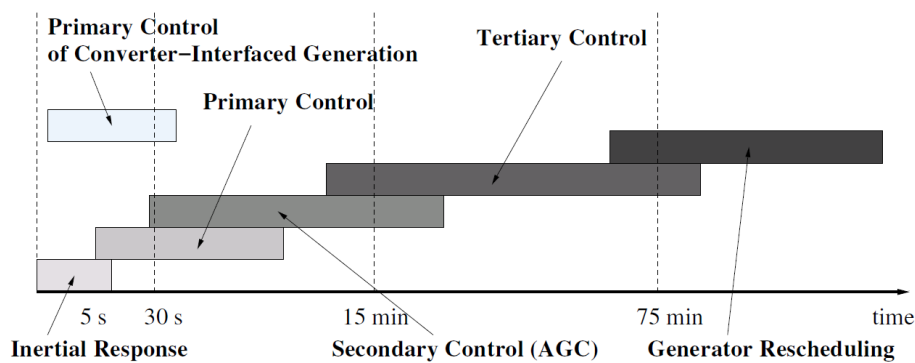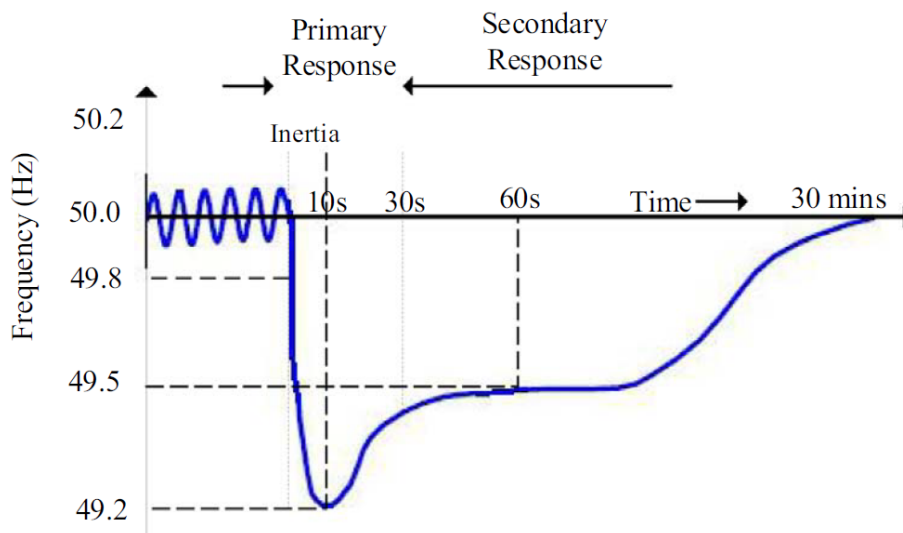
system inertia constant. After a contingency in the system, stored kinetic energy will be released in the form of active power when a shortage of generation takes place to avoid system frequency decay [25]. Contrarily, when there is an excess of energy in the system, frequency tends to increase and therefore, the rotating masses must absorb energy from the grid. This is the so-called Inertia Response. Additionally, when generation matches demand, frequency reaches its nominal value and no frequency deviation is verified.

2.3.2 Primary Frequency Control

In order to maintain the frequency at its target value, it is required that the active power produced and/or consumed could be controlled to keep the load and generation in balance. Therefore, a certain amount of active power, usually called frequency control reserve, must be available to perform this control within 30 seconds [2]. A positive frequency control reserve designates the active power reserve used to compensate for a drop in frequency and, on the other hand, the deployment of negative frequency control reserve is useful to decrease the frequency in the system [26]. Three levels of controls are generally used to maintain this balance between load and generation [15]. After the inertial response, primary frequency control, which is a local automatic control and the first stage in frequency regulation process, will be responsible for providing real power output by a generation unit in response to frequency deviation so that frequency could be stabilized in a few seconds after the disturbance [23]. For a steady-state frequency deviation Δf from the nominal frequency f_N, a generator that is participating in primary control will change its power generation by ΔP_G. In the case of a SG, frequency is generally not measured from the grid but through the rotation speed of the shaft because of its coupling with the grid. The droop S_G of this generator, which is the gain of the feedback loop in the primary frequency controller [26], is then defined as follows:

$$S_G = -\frac{\Delta f / f_N}{\Delta P_G / P_N} \qquad (2.12)$$

where

P_N is the nominal generator output power

Additionally, primary frequency control can adjust the consumption of controllable loads to restore quickly the balance between load and generation and counteract frequency deviations [15]. Thus, this first frequency control stage is indispensable for the stability of the power system. All the generators that are located in a synchronous zone and are fitted with a speed governor or governor-like action, which opens/closes the main control valves to increase/decrease the flow of working fluid through the turbine in order to increase/decrease the mechanical power output and consequently increase/decrease the active power injected into the grid [27]. Figure 2.4 shows a typical control system block diagram of a steam turbine.
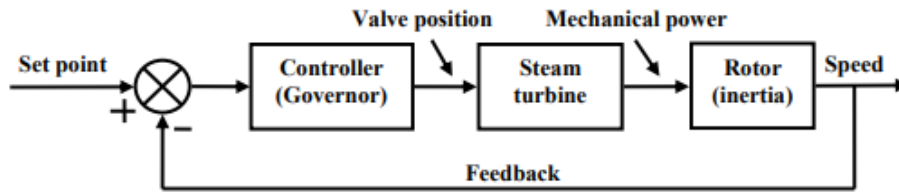
Figure 2.4: Speed steam turbine control [4]

Regarding primary frequency control, it is important to understand that the provision of this primary control is subject to some constraints. Some generators that increase their active power output in response to a frequency drop cannot sustain this response for an indefinite period of time. Their contribution must, therefore, be replaced before it runs out [26].

The demand side can also participate in this control through the self-regulating effect of frequency-sensitive loads such as induction motors [15] or the action of frequency-sensitive relays that disconnect or connect some loads at given frequency thresholds. However, this demand-side contribution may not always be taken into account in the calculation of the primary frequency control response.

2.3.3   Secondary Frequency Control

The instantaneous power output and power consumption are balanced, so the frequency is re-established by the primary control after a frequency disturbance. However, the re-established frequency is usually different from the nominal value. Therefore, secondary frequency control, which is a centralized automatic control, will be responsible for adjusting the active power production of the generating units, so that frequency and the interchanges with other systems could be restored to their target values following an imbalance [28]. In other words, while primary control limits and stops frequency deviations, secondary control brings the frequency back to its nominal value through the speed droop characteristics of the generators that are increased or decreased by the operators or by the automatic generation control (AGC). Therefore, the frequency can return to its reference value from 30 seconds to 30 minutes after a frequency disturbance [29]. Only the generating units that are located in the area where the imbalance occurred should participate in this control due to the responsibility of each area to maintain the match between load and generation.

Contrary to primary frequency control, secondary control is dispensable. This control is thus not implemented in some power systems where the frequency is regulated using only automatic primary and manual tertiary control. However, secondary frequency control is used in all large interconnected systems because manual control does not remove overloads on the tie lines quickly enough [26].

Additionally, the third stage in frequency regulation process is called tertiary frequency control and concerns to manual changes in the dispatching and commitment of generating units. This control is used to restore the primary and secondary frequency control reserves, to manage congestions in the transmission network, and to bring the frequency and the interchanges back to their

target value when the secondary control is unable to perform this last task. Some aspects of tertiary control relate to the trading of energy for balancing purposes.

2.4 Renewable Energy Sources in Isolated Power Systems

Over the last decade, RES participation in the electricity supply mix has constantly been increasing not only in interconnected power systems but also in isolated power systems. This power supply transition seeks to accomplish renewable-based electricity generation targets and policies as well as the de-carbonisation of societies for a more sustainable energy future. Such transition should be achieved through investments and consequent installation of wind and solar farms in power systems, not only because of their obvious environmental benefits but also because of their technological maturity and the consequent steady cost declining.

The Republic of Ireland is an example of an isolated power system with a steady increase of RES penetration, which according to [30], will increase its wind installed capacity to approximately 7692 MW (6892 MW onshore and 800 MW offshore) until 2030, compared to the 2272 MW of installed capacity in 2014 and an annual production of 17433 GWh is expected to be accomplished by wind generation. Additionally, in EU, a growth of almost 148% is expected to occur regarding wind installed capacity, compared to 2014 and wind generation will cover 24,4% of EU electricity demand [30]. Solar energy has been also subject to a large increase and thus, it is expected approximately 1270,5 GW of total global installed capacity in 2022 compared to 404,5 GW in 2017 [31].

Despite the renewable energy growth in several power grids, there are some technical challenges to deal with when we are in the presence of isolated power systems with variable RES. Those technical issues are identical to the ones faced by larger and interconnected systems, but they will be intensified in these less robust type of systems. Therefore, issues like frequency control and spinning reserve management become even more important to guarantee acceptable levels of stability and dynamic security in the system.

Moreover, the increasing participation of non-synchronous renewable sources in the generation mix, like wind generation and photovoltaics (PV), leads to a significant reduction in the amount of synchronous inertia present in the system, which is essential to avoid a rapid RoCoF and large frequency deviation after a contingency [32]. Unlike conventional generators, wind turbines and PV panels are connected to the grid through electronic inverters, establishing an electrical decoupling from grid [33] and, therefore, no inertia is provided to the grid making the system more fragile. Thus, higher RoCoF and frequency deviations will be observed, which might trigger the protection relays leading to a cascade of events/outages and to a blackout [24].

Therefore, there is an urgent need for wind turbines and PV systems to actively participate in frequency control like conventional power units, so that limitations to their penetration in generation mix can be avoided and at the same time system frequency stability is not put in risk. For that reason, new grid codes requirements have been defined in several countries for wind and solar power plants.

Regarding grid codes for wind generation units, the Great Britain Grid Code, for instance, requires that the normal deviation range of frequency in the system is from 49.8 to 50.2Hz. For this effect, all the wind power units must be capable of meeting all the frequency control requirements for primary and secondary frequency control. Therefore, when the frequency up to 10% of the rated system frequency, the wind power units are required to supply a primary frequency control which depends on their actual loading situation at the moment of the disturbance [34]. Additionally, the German Grid Code demands wind farms to reduce their power production when the system frequency is higher than normal values. The Grid Code also states that given a frequency deviation of ± 0.2 Hz, the primary response of the generating unit should be able to change by $\pm 2\%$ of the rated power output within 30 seconds and be preserved for at least 15 minutes. If the frequency rises to a value greater than 50.5 Hz, the TSO can ask for a reduction of the active power [34]. Therefore, future requirements could be imposed, such as: fast frequency support, which can be implemented via a temporary increase in power output immediately after a system frequency drop; inertia emulation, where a power converter is controlled in such a way that it injects power on the grid behaving as if it has inertia; virtual synchronous machines, which are power converters that emulate the operations of SGs and may provide inertia to the system, if local storage is available, and are also capable of providing fast proportional frequency response [35].

Regarding grid codes for PV power plants, the majority of the international grid codes for frequency have the same range between 47 and 52 to 53Hz. In Germany, the frequency variation range for PV power plants is between 47.5 and 51.5Hz otherwise, it must be disconnected immediately from the grid, with a clearance time of 0.2 seconds [36]. In the Chinese national gird, for instance, the normal operation range of frequency is from 49.5 to 50.2Hz, however, in case of frequency drop between 48 and 49.5Hz, the PV power plant must resist to this change for 10 minutes. Additionally, the PV power plant has to remain connected for 2 minutes if the frequency is greater than 50.2Hz otherwise, it has to be shut down [37].

Nowadays it exists a clear tendency towards more demanding requirements for wind and solar power plants, which is unavoidable and even desirable, as the penetration of wind and solar power in the generation mix is growing steadily. Wind and solar power plants developers and wind turbine as well as solar panels manufacturers are, therefore, increasingly facing similar requirements to conventional power stations. The adaptation process of grid codes for wind and solar power plants integration is not finished, and grid codes are expected to be developed further in the future. Moreover, improvements, especially concerning international harmonization of requirements, are expected to happen because many key aspects are unspecified at the moment [35].

2.4.1 Technical Challenges of Low Inertia Power Systems

Conventional SGs have been responsible for keeping frequency within certain technical limits, however, due to the steady replacement of online SGs by non-synchronous RES, which usually are types of converter-interfaced generation (CIG) makes the overall frequency regulation more

difficult for the system operator. Therefore, it is imperative that this type of generation can contribute to keep the system frequency within certain tolerated ranges. Otherwise renewable energy penetration must be limited.

The majority of CIG is non-dispatchable and modelled by stochastic processes, such as for wind speed and thus, these aspects can difficult the power dispatch and frequency regulation capabilities. However, their impacts are in these time scales larger than the inertial response of SGs. A large quota of non-synchronous generation comes from stochastic energy sources and, therefore, power unbalances are expected to be larger and more frequent when there is generation from non-synchronous power units, which is likely the reason why the penetration of RES is usually associated with the "low inertia power systems" issue. However, any non-SG will contribute to reduce the total inertia of the system, leading to increase frequency fluctuations [2].

Synchronous machines, on short time scales, affect the power balance by providing instantaneous physical storage through its kinetic energy stored in the rotating masses, but this is not enough for primary frequency control. Contrarily, for CIG, the instantaneous physical storage available is the energy stored in its DC-side capacitor, figure 2.5, which is negligible in comparison with the rotational inertia of SGs. However, power electronic sources can be actuated on much faster time scales than SGs, contributing to power balancing through their fast DC energy supply and therefore, the lack of physical inertia can be compensated through their fast DC-side energy storage system (ESS), like batteries, flywheels or super-capacitors [2].
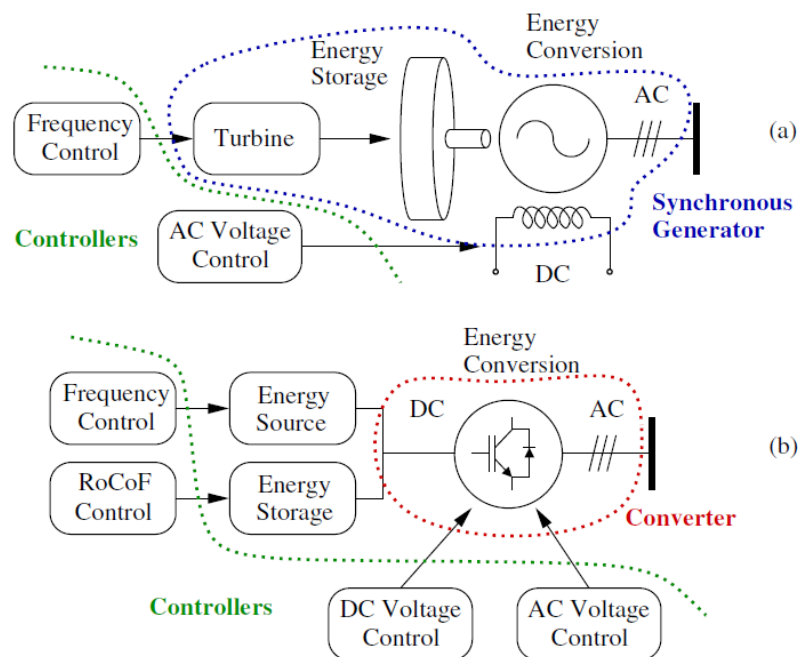

Figure 2.5: Energy conversion, storage and controllers of synchronous machines (a) and power electronic converters (b) [2]

As mentioned before, power converters are usually fast and allow non-SGs to provide a primary frequency control faster than conventional power units [38, 39], however since power con-

verters do not respond to power unbalances in a natural way, the very first moments after a contingency might not be fully covered, which is where the inertial response of SGs has its most important impact on system dynamics. Additionally, the reserve and thus, the ability to help in primary frequency control by CIG is limited [40]. This is because CIG is usually operated at its maximum power point (MPP) for energy and economic benefit. Even if CIG is operated with a certain reserve, the problem will persist due to the stochastic nature of most CIG, which prevents guaranteeing a given reserve and security margin to the power system.

Non-SGs do not respond to power variations unless forced to by a specifically designed control loop which is subject to delays, malfunctioning, saturation and unexpected coupling with other dynamics possibly leading to instabilities [2]. A 100% non-synchronous generation penetration is not a realistic scenario for large systems at least for the time being. However, it is possible that, for short time periods, the percentage of non-synchronous generation can be very large when the grid is isolated. In a 100% non-synchronous generation penetration scenario, the variation of the frequency is immaterial for the determination of the power imbalance, where, in equation 2.8 the total inertia of the synchronous machines is null, leading to the total decoupling between frequency and power balance. This has led many researchers to find new techniques to balance the power through controllers that do not need to measure the frequency [41, 42]. Nevertheless, this type of controllers tend to rely on communications systems and are not fully reliable nor easy to implement and, at the moment, there is no clear alternative to substitute the frequency as the main signal to regulate the power balance, which turns difficult the 100% instantaneous penetration of non-conventional generation [2].

The primary frequency control of the SGs is based on the measure of the rotor angular speed of the machine itself since the dynamic response of this type of machine leads to frequency variations and therefore, the rotor speed is naturally the right measurement to use for frequency regulation. However, when it comes to CIG, the situation is different, which depending on the mode of operation does not necessarily impose the frequency at the point of connection. In this situation, the local bus frequency is a fragile signal that needs to be estimated through available measurements, such as AC voltages at the point of connection and the outputs of the Phase-Locked Loops (PLL), which are devices that usually are used for frequency deviation estimation and to enable grid-connected power converters to maintain synchronous with the grid. However, PLL can present numerical issues and provide a frequency estimation affected by discontinuities and high-frequency noise. Moreover, PLL introduces a non-negligible delay that can limit the performance of the controllers that rely on the frequency estimation of the PLL system [43–46].

Some solutions to these challenges have been studied, like the idea of RoCoF detection through the use of frequency locked-loops (FLLs), which can avoid high-frequency noise amplifications introduced by differential operations [47]. Virtual-synchronous-controlled (VSynC) and DFIWG synchronizing techniques that make DFIWG synchronize with power grid through the active power control (APC) are other solutions [43]. Moreover, considering a unique frequency for the system usually referred to the frequency of the centre of inertia (COI), it is possible to obtain an overall smoother frequency response and better control provided by CIG than PLL estimations by

using a COI signal [2]. However, this signal is not usually measured by system operators due to the necessity of measurements of all synchronous machines rotor speeds in the system.

Some issues have been raised about converter modelling. In a low inertia power system, there is a need to have an accurate representation of power electronic converters, their limitations and their controls, mainly on the short time scales [2]. The literature highlight the effects of control lags and measurement delays, especially of PLLs, as the dominant dynamics of power electronics sources. In [48], the dominant converter DC charge dynamics of a converter and their analogy to the mechanical swing dynamics of a synchronous machine is highlighted. However, this analogy is only formal, as the energy stored in the DC capacitor is negligible with respect to that stored by the inertia of SGs. To make this analogy viable, it is necessary to connect a sufficiently large energy storage device to the DC side of the converter [2], figure 2.5. Additionally, in order to respond to the variation of frequency, while the mechanical inertia is an inseparable part of the SG, converters require fast DC-side energy storage and specific control.

Another important issue that must be considered is the fact that the amount of inertia present in the power system will become dependent on the generation mix dispatched for a particular time with the steady replacement of SGs by non-synchronous machines. Therefore, the system inertia becomes time-dependent and a function of expected solar and wind power output because these two power sources determine the amount of energy that must be provided by conventional power plants to cover the remaining net load [2]. Moreover, utilities are considering to find market solutions to establish a sufficient level of inertia in the system, which indicates that is necessary to model system inertia as a time-dependent variable that must be included as a lower-bounded variable into the mathematical dispatch modelling [2].

As mentioned before, the lack of natural dynamics and interaction with the grid by CIG, as a result of a missing coupling between grid and the CIG, the interaction of these sources with the grid is determined by the chosen control methodology.

In current power systems, two common operation modes of low inertia sources are the grid-following or grid-feeding mode and the grid-forming mode [49–52]. In the grid-following mode, the CIG stays synchronous and provides an amount of power simply following the imposed frequency and voltage that are regulated by the grid. In the grid-forming operation mode, the CIG regulates the frequency and the voltage at its terminal, similar to a SG. Therefore, it is only possible to operate CIG in grid-feeding mode if there are other resources that do form frequency and voltage. However, with the steady increase of RES penetration connected through power electronics, it is required that some of these will be operated in grid-forming mode in order to provide not only a reference and support for frequency and voltage but also to provide black-start capabilities and a robust and stable synchronization mechanism [2]. Consequently, considering all the potential operating modes, trying to understand in what mode each converter in the system should operate and how many of them must be operated in grid-forming mode, becomes imperative.

The transition from grid-following to grid-forming converter operation mode is a control problem. The solution lays on the designing of grid-forming converters by emulating synchronous machines, as well as their inertial response and their control mechanisms. Virtual inertia emulation

techniques are based on measurements of AC quantities such as frequency and injected power [2]. Nevertheless, it is important to notice that for virtual inertia emulation purpose, there is a complex signal processing methodology which is responsible for increasing the complexity and the actuation delay in the control loop. Additionally, the converter current limits during a post-contingency dynamics could be another limitation [53].

Regarding low inertia power systems changes and solutions, the most relevant questions are concerned with how non-conventional power sources are interfaced with the larger utility grid. The general limitations of converter control have already been mentioned, as well as several control approaches. Although these strategies are successful and viable under nominal conditions, they have limitations for post-contingency stabilization. Therefore, it is expected that due its simplicity, droop control be subjected to more research to become more robust and more widely applicable [2]. Additionally, matching control [48], as well as virtual oscillator control are two control strategies that have been studied so that grid-forming mode control could overcome such limitations.

Moreover, as already discussed, PLLs are sensitive to noise which can cause instabilities and therefore, techniques based in PLLs might be inadequate for synchronization of many generation units in a low inertia power system. The replacement of the PLL with a controller that emulates the self-synchronizing nature of an induction machine [54], as well as substitute the PLL with a virtual synchronous machine emulation [55] and the modification of the existing synchronverter control strategy in order to provide self-synchronization are some of the actual options [56]. Another alternative to obtain the information of frequency balance in a converter-based system can be derived from the matching control principles, where the voltage measurement on the DC side of a converter can equally indicate the instantaneous power imbalance [2].

2.4.2 Inertia Emulation

The increasing penetration of wind energy sources and PV has decreased the inertia constant of power systems due to the decoupling of the RESs from the AC grid using power converters and made them inverter-based. This makes the modern grid susceptible to frequency instability when facing generation-load imbalances, leading to triggering under-frequency load shedding (UFLS) followed by cascading failures, which may damage equipment and further lead to blackouts [57]. In normal operation, RESs cannot participate with other conventional generation sources in frequency regulation. Therefore, many inertia and frequency control techniques have been proposed for variable speed wind turbines and solar PV generators. Generally, the inertia and frequency regulation techniques are divided into two main categories. The first one includes the deloading technique, which allows the RESs to keep a certain amount of reserve power, while the second one includes inertia emulation, fast power reserve, and droop techniques, which is used to release the RESs reserve power when under frequency events occurs. Additionally, different inertia and frequency control techniques for RESs with and without ESS (batteries, supercapacitors or flywheels) can be considered.

ESSs have the ability to inject and absorb power, behaving as energy suppliers or consumers and, therefore, be used for many purposes in the grid such as peak shaving, voltage regulation, and even as backup power. When it comes to power balance and frequency response, ESSs, characterized by its fast-ramping, and also deloading of wind and PV, can work along with control algorithms and power electronics to emulate the inertia of a conventional power system and provide virtual inertia to the system [58]. However, ESSs have some technical issues that need to be analysed. One of the most important is their ageing. When working as a resource for frequency response, batteries, for instance, are exposed to several charging and discharging cycles, which directly impacts their lifetime and brings extra costs to ESSs owners [58].

Virtual inertia emulation is a solution in which the output power of RESs is controlled, in some cases, based on the ROCOF of the system. This type of power sources have typically been integrated as grid-following units [59] and do not contribute to the inertia of the system. However, some control algorithms that emulate virtual inertia have been proposed, like in [60–62]. In [60] the rotor inertia is emulated through the usage of a short-term energy buffer which is added to the system and be controlled at a fast rate, creating the so-called Virtual Synchronous Generator (VSG). Additionally, in [61] it is exploited a technique where a VSG has an alternating moment of inertia, and in [62] it is proposed operating an inverter to mimic a SG (Synchronverter). All these control algorithms have shown significant improvements in system stability. Therefore, virtual inertia systems should play a crucial role in the growth of RES penetration in power systems while maintaining reliability and security 2.6, where its deployment will be driven by the technical requirements of the grid and market needs [57].
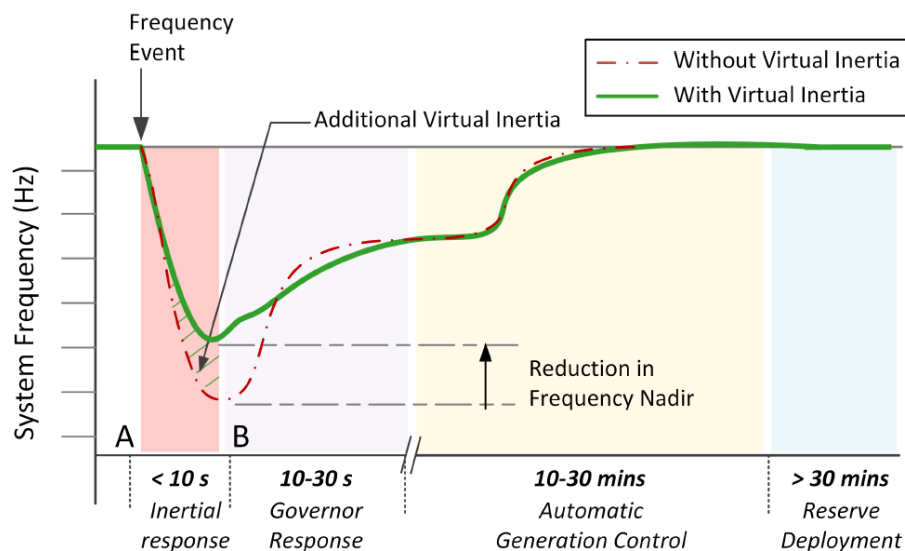

Figure 2.6: Frequency control stages with and without virtual inertia [5]

2.4.3 Wind Turbines Participation in Frequency Control

Power systems are facing a large wind generation penetration, which may lead to difficulties in frequency regulation. However, some technological solutions are allowing wind turbines to participate in frequency control and thus providing an increase in system robustness and security. Moreover, the contribution of wind turbines to primary frequency control is nowadays required by several grid operators, especially during valley hours but it is a difficult task as the energy source is not controllable [63].

Two main categories of wind turbine are used for energy production, they are: the fixed speed and the variable speed turbines [40]. The first one generally uses an induction generator that is connected directly to the grid and can provide an inertial response when a frequency deviation occurs, even though this inertia is negligible compared to the SG. A variable speed wind turbine mainly uses a Permanent Magnet Synchronous Generator (PMSG). The PMSG is totally decoupled from the grid, due to the stator of this type of generator is connected to the power electronic converter, so that power could be injected into the grid. The DFIG is similar to the PMSG, except for the fact that this generator is connected to the grid via a rotor circuit. The power electronic converter used in a variable speed wind turbine enables the wind turbine to regulate the output power over a wide range of wind speeds [64]. However, this coupling isolates the wind turbine from the frequency response under disturbance. Additionally, traditional wind turbines are operated under a strategy that allows the maximum energy extraction from the wind flow and therefore, they do not have reserve power to support frequency control.

Considering this, researchers have investigated two main techniques to support frequency control without ESSs using a variable speed wind turbine, inertia response, and power reserve control. Inertia control enables the wind turbine to release the kinetic energy stored in the rotating blades within few seconds to arrest the frequency deviation, while reserve control technique uses the pitch angle controller, speed controller, or a combination of the two to increase the power reserve margin during disturbances.

Wind turbines do not have the same ability as conventional generators have for automatically release the kinetic energy stored in their rotating blades. Consequently, the wind turbine needs a suitable controller to provide inertia response. There are two control techniques for that purpose: inertia emulation and fast power reserve [7]. Inertia emulation proposes new control loops for power electronic converters, based on ROCOF and frequency deviation measurements, to release the kinetic energy stored in rotating blades of wind turbine and it is used to arrest frequency deviation during power unbalances. Fast power reserve can also be used to arrest frequency deviations however, this technique responds to frequency deviations by releasing constant power for an amount of time, for instance, 10% of the nominal active power during 10 seconds [7].

For the inertia control, it is developed in [65] a supplementary control loop which is added to the DFIWG controller in order to provide inertial response, figure 2.7, something that DFIWG could not do before due the fact that DFIWG control system decouples the mechanical and electrical system and therefore, frequency deviations cannot be seen by the generator rotor. This strategy

uses the kinetic energy stored in the rotating mass of the wind turbine, so that the additional amount of power supplied by the wind generation unit to the grid is proportional to the derivative of the system frequency, as follows:

$$P = \frac{dE_k}{dt} = J\omega\frac{d\omega}{dt} \tag{2.13}$$

which can be written, in per-unit, as

$$T = 2H\frac{d\omega}{dt} \tag{2.14}$$

Equation 2.14 is the signal that is added to the controller. When the system frequency starts to drop, the setpoint torque is increased, slowing the rotor and extracting kinetic energy. Moreover, results in [65] show that this controller allows DFIWG to provide more kinetic energy than fixed-speed wind turbines. This inertial control method attempts to create an artificial wind turbine inertial response.
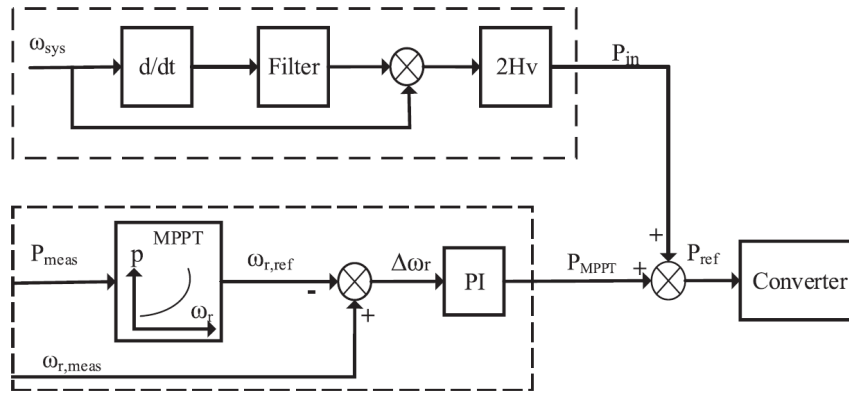
Figure 2.7: Control loop for inertia emulation by variable speed wind turbine [6]

Regarding fast power reserve, which is one type of inertia response control, the inertia response can be emulated, as the control signal depends on the frequency deviation or ROCOF. It can also be defined as a constant 10% of the nominal active power during 10 seconds, despite different wind speeds [66]. The short-term constant power, which is called the fast power reserve, is released from the kinetic energy stored in the rotating blades of the wind turbine. This fast power reserve can be achieved by controlling the rotor speed set point. This is given by:

$$P_{const}t = \frac{1}{2}J_{\omega ro^2} - \frac{1}{2}J_{\omega rt^2} \tag{2.15}$$

where

P_{const} is the constant amount of active power

t is the time duration for the fast power reserve

ωro^2 is the initial rotational speed

ωrt^2 is the rotational speed at the end of inertial response

Thereby, the reference rotational speed can be obtained by:

$$\omega r, ref = \omega rt = \sqrt{\omega ro^2 - 2\frac{P_{const}}{J}t} \qquad (2.16)$$

Moreover, the fast power reserves compensate the power loss during a short period of time and give more time for other slower generators to participate in the frequency control [67].

Another technique used for inertia emulation by wind turbines without ESS is th droop control, which control the active power output from a wind turbine proportional to frequency change. This controller improves the frequency nadir as well as the frequency recovery process following disturbances. The active power is adjusted according to linear characteristics and is given by:

$$\Delta P = P1 - P0 = -\frac{f_{meas} - f_{nom}}{R} \qquad (2.17)$$

where

R is the droop constant

f_{meas} is the new frequency

$P1$ is the new wind turbine output power

f_{nom} is the initial frequency

$P0$ is initial power output

The linear relation between frequency and the active power of the wind turbine is illustrated in figure 2.8.
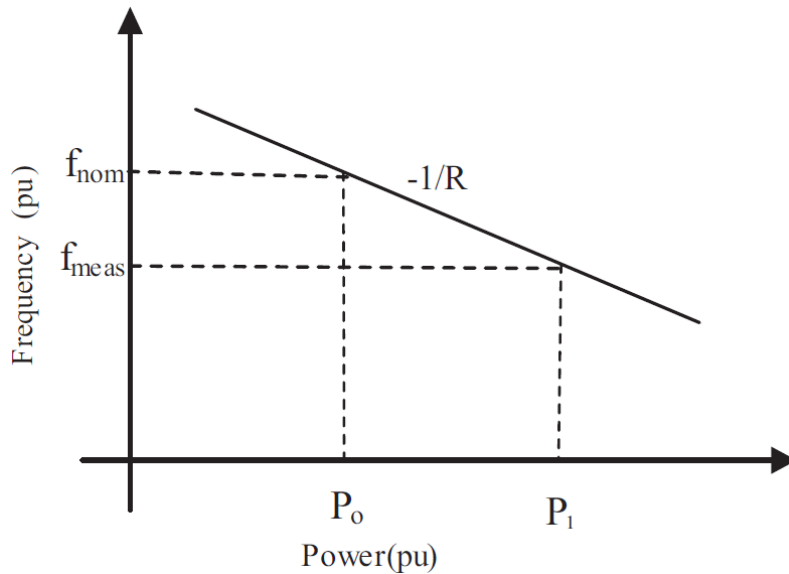

Figure 2.8: Droop characteristics of a wind turbine [7]

Droop control can be implemented in the converter of a variable speed wind turbine. However, the power increase ΔP, that is absorbed from the kinetic energy leads to the rotational speed decrease due to the MPPT operation of the wind turbine. Therefore, the turbine may stall if the rotational speed becomes to slow. This may occur because the wind turbine cannot provide extra permanent power to reduce the frequency deviation [68]. Additionally, another application is to use the droop control with the deloading control that is explained next.

In order to maximize the economic benefits, wind turbines are designed to operate on an optimum power extraction curve to extract the wind energy as much as possible. As a result, they do not participate in frequency regulation because there is no power margin. For this reason, sufficient reserve capacity must be available in the system to address any frequency deviation. Deloading control techniques ensure a reserve margin for the long-term frequency control by shifting the wind turbine's operating point from its optimal power extraction curve to a reduced power level [7]. Considering the wind turbine's aerodynamic behavior, the mechanical output power captured by the wind turbine will be obtained by:

$$P_m = \frac{1}{2}\rho A C_p\left(\lambda,\beta\right)v^3 \tag{2.18}$$

Where ρ is the air density, A is the rotor sweep area, v is the wind speed; C_P is the power coefficient, β is the pitch angle and λ is the tip speed ratio, which is given by:

$$\lambda = \frac{\omega_r R}{v} \tag{2.19}$$

It is clear that the output power of the wind turbine is dependent on the pitch angle β and the tip speed ratio λ. Therefore, the deloading technique has two types of control system: the speed control and pitch angle control. The active power can be modified by controlling the pitch angle from β_{min} to a larger value $\beta 1$ for a constant wind speed $V_{\omega 0}$ and constant rotational speed. Additionally, the power can also be changed by increasing the rotational speed over the MPPT speed for a constant wind speed $V_{\omega 0}$ and a constant pitch angle β_{min}, figure 2.9.
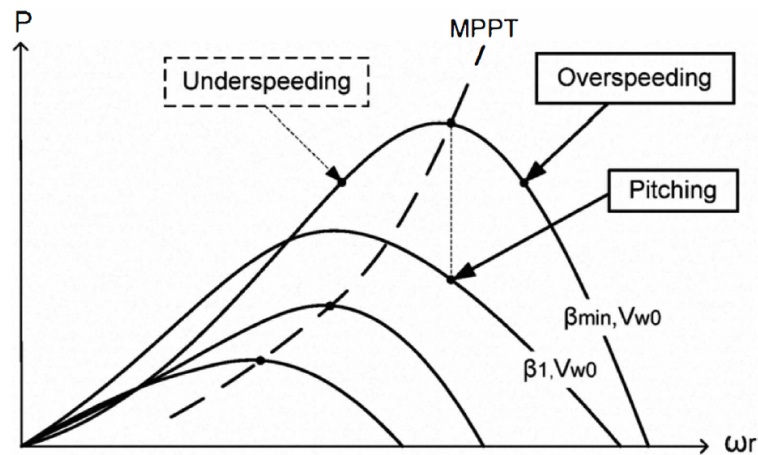

Figure 2.9: Pitch angle control and speed control techniques [6]

Decreasing the rotational speed below the MPPT speed is, in fact, a deloading possibility. However, while over-speeding improves the small signal stability, under-speeding may decrease the small signal stability compared with pitching [69]. Meanwhile, the rotor has to firstly absorb extra energy from the grid and increase the rotational speed, which may lead to a second frequency drop. Therefore, over-speeding is a better approach [70, 71].

Inertia control can also be similar to the one usually used in conventional SG as presented in [8]. The droop loop is used in order to produce a variation in the active power that is injected by the wind generator, being proportional to the difference between the measured and the nominal frequency, as follows

$$P_{inj} = P_{ref} - \frac{1}{R}\left(\omega_{sys.meas} - \omega_{sys.nom}\right) \tag{2.20}$$

where

P_{inj} is the injected active power

P_{ref} is the active power reference

R is the droop control regulator in p.u.

$\omega_{sys.meas}$ is the measured system frequency

$\omega_{sys.nom}$ is the nominal system frequency

This control strategy uses an additional frequency control loop that is integrated into the rotor-side active power controller of the DFIWG [8], as shown in figure 2.10.
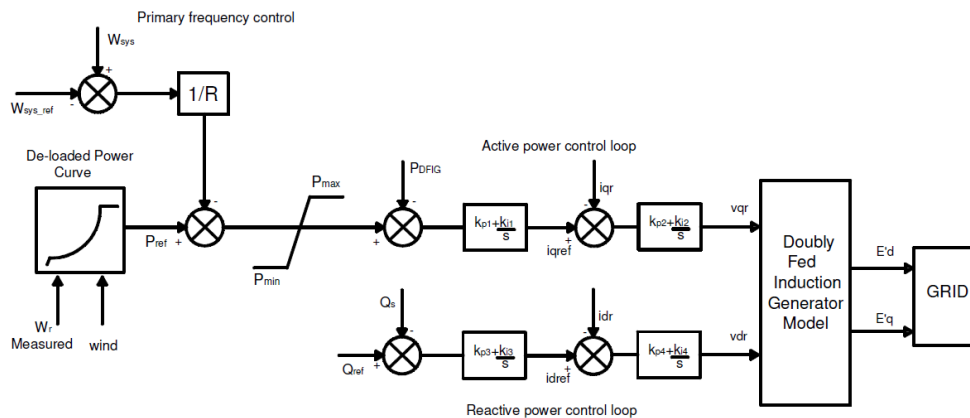
Figure 2.10: Rotor-side controller for primary frequency regulation [8]

In this control strategy, a deload regarding the maximum power extraction curve of the wind generator is used to allow its contribution in frequency regulation during a system frequency drop, by giving to the wind turbine generator a margin to increase the active power injected into the grid. Additionally, a pitch control strategy is included and masters the power control for high wind speeds. Basically, for wind speeds larger than the maximum rated speed, the blade pitch control limits the energy extracted by the turbine. Therefore, the pitch angle control will control the rotor speed and will operate until the wind cut-off speed limit is reached [8]. A combined

operation of the pitch control and the electronic converter control should be used in a large deload scenario, as described in [72]. This strategy allows an active power injection from the DFIWG when the system frequency falls by decreasing the pitch angle as system frequency drops so that the turbine can extract more mechanical power from wind flow.

It is also exploited in literature a frequency regulation strategy that combines both frequency control schemes described before. In [63], besides the original methodology where wind generators do not supply the maximum available power so that a margin remains for frequency control, an additional control is proposed in order to wind turbines can provide virtual inertia to the system.

In this strategy, the controller of the variable speed wind turbine (VSWT) gives a torque setpoint that is based on measured power and speed. This torque set point signal is the input for the converter control that realizes the torque by controlling the generator currents [63]. However, this frequency control approach adapts the torque setpoint as a function of the system frequency deviation and the grid RoCoF. In this approach, the primary frequency control is activated when the frequency of the system exceeds certain limits.

When the inertial control mode is exploited, wind generators are not capable of participating properly in the system primary frequency control because they are not deloaded and, as mentioned before, no active power margin exists to provide extra power when frequency decreases.

In [73], a primary frequency control technique has been developed, so that DFIWG is able to provide frequency response, by using a pitch angle controller to deload the power output. With this technique, the active power injected by the wind generator is adjusted through the regulation of the minimum pitch angle according to frequency deviation [73]. Moreover, this type of control is used for both fixed speed induction wind generator (FSIWG) and DFIWG, however, in the last one, this control is operated alongside with the power electronic controller [73].

Additionally, a primary frequency control approach for a DFIWG is presented in [9] where a combination of control of the static converters and pitch control is exploited. In this type of control, wind generator operates according to a deloaded optimum power extraction curve to provide active power during a frequency deviation, by adjusting the rotor speed. When a frequency disturbance occurs, the action of the rotor-side electronic converter of the wind generator will lead to an active power injection followed by the pitch control so that mechanical power could be adjusted. The electrical power injection is defined from a proportional frequency control loop alongside with a power reference adjustment resulting from a deloaded power curve so that a new equilibrium point can be reached when a frequency deviation takes place [9].

The active and reactive power control loops, as well as a primary frequency control loop, a pitch control strategy and a control block concerning to a external supervisory wind park control system are included in the control technique adopted for the rotor-side converter of the DFIWG. The primary frequency control included in the rotor-side control loop consist in a droop loop, whose purpose is try to emulate the proportional primary frequency control strategy used in a conventional SG [9]. Furthermore, this control is completed by the pitch angle control, used simultaneously with the static converters, by adapting the rotor speed according to the deloaded maximum power curve, figure 2.11.
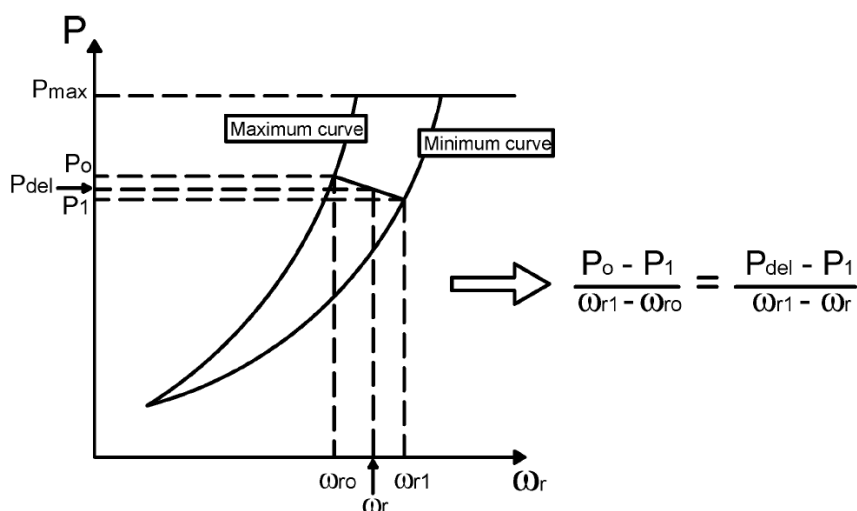
Figure 2.11: Deloaded optimal power curve [9]

Another strategy used to deload the wind turbines is operating them at increased speed and select a power-rotational speed (P-ω) setting different from the optimum [74]. This strategy is based on varying the (P-ω) curve depending on the system frequency and, therefore, to increase the wind turbine power output, the speed has to be decreased and vice-versa. This method is called the speed control for primary frequency regulation.

The majority of frequency control strategies of a wind turbine are currently designed to have a new control loop like droop control, pitch angle control or speed control, as seen throughout this section. However, these control loops have some disadvantages and could not solve the issues of frequency control properly. For instance, pitch angle control may not have a fast-speed response capacity to help in frequency support when the system frequency starts to fall and speed control can only work under the rated wind speed [34].

Moreover, the inertial control from wind turbines allows a temporary overload of the machine in terms of current and voltage, when operating at high wind speeds [75]. Additionally, the kinetic energy storage system used to participate in primary frequency control by the inertial control can only be considered as a part of primary control because this power reserve cannot be assured further to short-term [74]. Standard methods to enable frequency regulation by wind turbines are needed as well as more research to determine the best approach for specific systems in order to reach the most effective frequency control by wind turbines [34].

Different control techniques have been proposed so that RESs could regulate system frequency during disturbances. However, these techniques have some issues in terms of reliability, as the nature of the RESs depends on variable and non-controllable factors. Therefore, ESSs should work with variable speed wind turbines or solar photovoltaic to increase the reliability of frequency regulation [7].

In [76], cooperation between frequency control techniques and ESS was proposed for the DFIG wind turbine. This approach helps to overcome some problems of frequency control tech-

niques, such as second frequency drop and oscillations. In fact, the ESS has two main functions in supporting frequency regulation in all wind speed ranges. In the first one, the ESS provides the active power required for speedy recovery, so that second frequency drop could be prevented, while in the second, the ESS is used as a backup system for the provision of power during deficits. In [77], primary frequency control was used in wind power plants to keep a certain level of power reserve. The wind power plant is supported by a flywheel storage system to guarantee the power reserve requirements set by the system operator. In steady-state conditions, a central controller distributes the power reserve requirement between the wind turbines and the flywheel storage system and the power reserve margin is determined depending on the wind speed range.

Moreover, in [38], a virtual inertia technique was proposed for the DFIG wind turbine to provide short-term frequency response. However, since this technique focuses on short-term oscillation, there is no need for long power regulation, and therefore, a super-capacitor is connected to the DC-link of the DFIG wind turbine inverter via a DC-DC converter. It is showed in [38] that using the DFIG rotating mass or super-capacitor as the virtual inertia source improves system stability. However, each type has different impacts. Although the super-capacitor virtual inertia can enhance system stability and is independent of wind speed, it requires new components. On the other hand, the rotating mass virtual inertia does not require additional components, but its performance is highly dependent on wind speed variations.

2.4.4   PV Systems Participation in Frequency Control

As the initial installation of PV systems is relatively costly, these type of systems are designed to operate in their MPP region in order to maximize energy benefits and income. However, adopting this PV systems exploitation strategy will not allow PV systems to actively contribute in system frequency regulation due to the fact that no generating margin is preserved to improve the frequency response by releasing excess energy during under-frequency events [78–80].

Therefore, some strategies and techniques have been studied and implemented so that PV panels can contribute to frequency control. Some of them can be exploited through the usage of ESSs or the deloading technique without ESS. Operating a PV system below MPP; installing and operating an ESS while keeping the PV system in the MPP region; installing and operating a dump load bank to absorb excess energy [80], are some of the strategies to be considered.

Shifting the PV system operation point below MPP consist in operating a PV in a power dispatch mode by some deliberate curtailment strategies so that a generating margin is created to contribute to frequency regulation. Figure 2.12 shows a deloading technique, which is attained by increasing the PV voltage beyond the MPP voltage. This is possible by increasing the value from V_{MPP} by voltage V_{deload}, allowing the PV array to keep some reserve power. Thus, this reserve power will not be released until the system frequency deviates. Under these conditions, it is added to the DC reference voltage, a control signal proportional to frequency deviation $V_{dc\Delta f}$. It is shown in figure 2.12 that the change in output power from the PV will depend on the V_{MPP} value and the frequency deviation, as given by equation 2.21.

$$V_{dcref} = V_{MPP} + V deload - V_{dc\Delta f} \qquad (2.21)$$
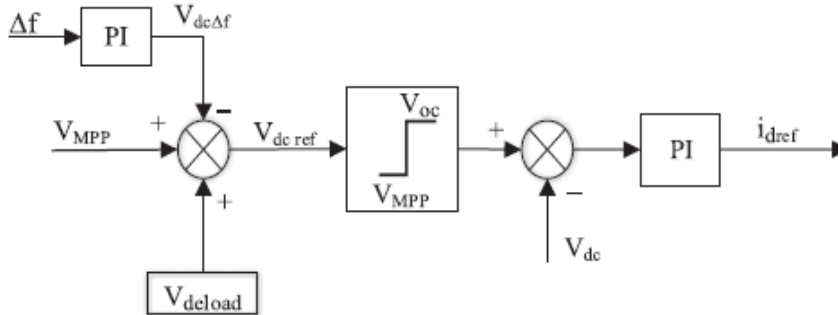
Figure 2.12: Deloaded PV system controller [10]
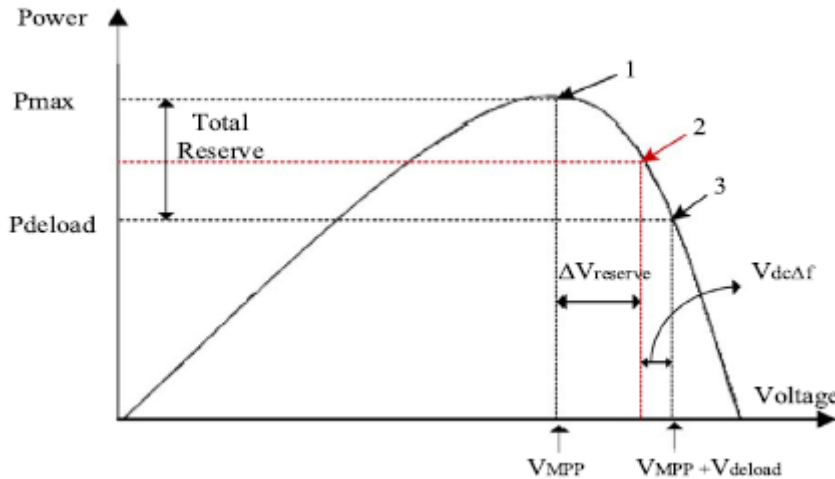
Figure 2.13: Deloaded PV system strategy [11]

The operation of the deloaded controller is shown in figure 2.13, where PV system is working at point 3 to keep some reserve power. This situation continues until the system frequency starts to drop, at which point, a control signal related to frequency deviation will reduce the PV voltage, and make the PV work at point 2. However, the controller does not take into consideration the remaining reserve power for each PV unit. Therefore, all PV units will release the same amounts of active power needed for frequency regulation, even if the reserve power of each unit will not be equal. As a result of this, some PV units with fewer reserves will reach the MPP faster and will not be able to keep its contribution to frequency regulation, leading to the non-uniform distribution of frequency regulation [7]. It is proposed in [11] a variation to the previous controller by adding a new control signal representing the remaining reserve power. The reference voltage of the new controller shows, equation 2.22, that the output power released from the PV units is not equal, and depends on the reserve power available for each one.

$$V_{dcref} = \left(V_{MPP} + Vdeload - V_{dc\Delta f}\right) - \left(\Delta f \times \Delta V_{reserve} \times K_{P2}\right) \qquad (2.22)$$

In [81], two new algorithms were implemented, enabling a solar PV system to control frequency. The first one was the traditional MPPT controller, which is responsible for operating the PV system on MPP during normal operations. For transient conditions, a control signal would activate the deloading algorithm, which uses a modified fractional open circuit voltage. This modification proposed the usage of the ratio K as a controlled variable, which determines the amount of reserve power for PV systems limited to the range (0.8–0.95) [7]. The main conclusion of this work shows that a PV generator cannot control the frequency but also to follow load changes.

In [79], a fuzzy-based control strategy is proposed, enabling PV system to contribute to frequency regulation without any ESS. Basically, with this strategy, the PV system is forced to participate in inertial response only when the system inertia is not satisfactory. Thus, this control has the frequency deviation and system inertia as input and the output decides the operating point to provide primary frequency response.

Moreover, another control technique designed for PV systems without ESS is the dump load technique. This technique consists of a resistance and a controller used to control the power that flows through the load. The purpose of the dump load is to absorb the excess power generated from the PV system, and thus, to smooth the power injected into the grid [82]. Additionally, the load can be cooled to avoid excessive heating during its operation.

However, it is important to understand that these strategies usually leads to revenue losses by the PV owners, who need to be encouraged to operate under deloaded condition by compensating them for the income losses in power generation [82].

Another approach regarding frequency support by PV systems lays on the usage of an ESS such as batteries, ultracapacitors and flywheels. All these solutions can provide primary support in case of any disturbance, although they have some technical issues that need to be analysed. Batteries have a quick response in charging and discharging process (some batteries can respond to load variations in about 20 milliseconds [83]) as well as high energy density and moderate cost, making them suitable for frequency control and for reducing power fluctuation in PV systems. However their lifetime could be a limitation by not being able to provide the repeated charge/discharge cycles that are required in many energy storage applications [83]. For that reason using batteries with ultracapacitors can be a possibility in order to overcome their technical limitations. Ultracapacitors have high power density, high efficiency and can be cycled tens of thousands of times and have a much faster charge and discharge capabilities than batteries but have a low energy density, which limited their use for only applications that requires small quantities of energy before the ultracapacitors can be recharged [78]. Therefore, using it with batteries will prove advantageous.

In [84], a frequency and voltage control technique using Li-ion batteries coupled to the grid is presented. This technique allows effective control over the active and reactive power available from the system, allowing the system to participate in frequency regulation. For an up-regulation, the PV/battery system injects active power into the grid and, for a down-regulation, the storage

battery absorbs the output power from the PV system and excess power from the grid.

Flywheel energy storage system consists of a massive rotating cylinder, where steel wheels increase the rotating inertia, and it is very commonly used not only to improve the quality of the generated power but also to support critical loads during power interruption because of its simplicity of storing kinetic energy in the spinning mass [85]. There are two types of flywheels, the low-speed flywheel (up to 6000 rpm) with higher power density and the high-speed flywheel (up to 60000 rpm) that has a higher power and energy density due to the usage of advanced composite wheels [85]. The usual configuration of a flywheel consists in an electrical machine that drives the flywheel, and its electrical part is connected to the grid through a back-to-back converter. For frequency support purpose, when an excess of energy production is verified due to the power imbalance in the system, the flywheel will be driven by the electrical machine operating as a motor and the excess of energy will be stored in the flywheel. Contrarily, when a lack of energy is verified, the electrical machine is driven by the flywheel and will be operated as a generator so that extra energy could be supplied [83]. Usually, the efficiency of flywheel solution is between 80 and 85%, and researchers are now focusing on increasing energy and power density with new designs, improving the cooling systems that are responsible for removing heat from the wheel [83].

In [82] is concluded that combining an ESS with the below MPP point operation is the best cost-effective solution and in [11], the deloading of a PV unit is more economically advantageous than using a battery.

2.5   Synchronous Condensers

SC have been played an important role to support electric power systems in terms of voltage stability and contribution to short-circuit capacity of the system [86]. However, due power electronic solutions like STATCOM and Static Var Compensators (SVC) has lower capital costs and maintenance level (these do not have rotating parts), SC have been replaced by these technological solutions for voltage control purpose [87].

Nevertheless, because SC are a rotational unloaded synchronous machines, they can provide inertia to the grid through the kinetic energy stored in its rotating mass. Active power is released and absorbed from the grid when, for instance, a generator is suddenly tripped, or load level decreases respectively in order to eliminate power unbalance and guarantee the dynamic security of frequency control [23]. This is called the inertial response, which is followed by primary and secondary frequency control.

Therefore, the decline of conventional power generation units and consequent increasing penetration of non-synchronous generation in power systems over the last few years brings significant impacts on system frequency behavior, which may suffer stronger and faster deviations during a contingency. To address this issue, SC are installed in the electric networks to provide extra inertia to the system, figure 2.14, making it more robust to face possible contingencies better and avoid that frequency stability of the system be easily jeopardized.
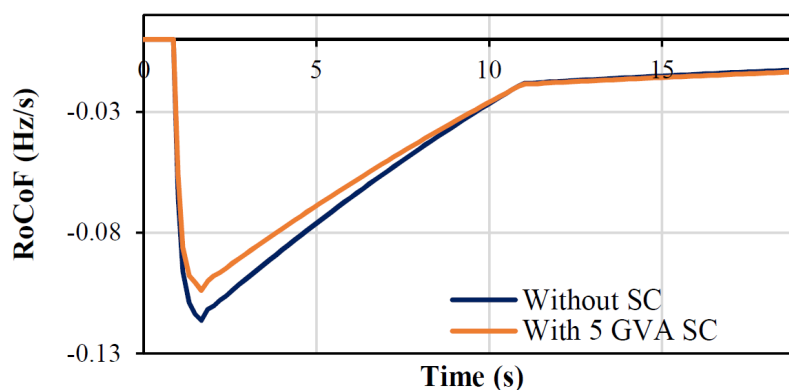
Figure 2.14: RoCoF with and without SC installed [12]

2.6 Dynamic Security Assessment

Dynamic security assessment of a power system concerns two main objectives: first, to evaluate the system's capacity to withstand major disturbances, and second to suggest corrective actions to enhance this capacity, whenever needed. The first objective is the concern of analysis, the second is a matter of control [88]. It is used to determine which contingencies may cause power system limit violations or system instability and includes different forms of stability assessment, such as: rotor angle stability; voltage stability and frequency stability. However, frequency stability is generally associated with the behavior and security of islanded power systems, playing an important role in the secure and reliable operation of the systems. Traditionally, dynamic security analysis has been conducted in an off-line planning environment using power flow, step-by-step time domain simulations based on forecasting and extensive contingency simulations to cover a wide range of possible system conditions [89]. Even if advanced computers were used, this simulation methodology could be very slow, and it cannot give the stability margin and sensitivity information, which is essential to determine power transfer limits and corrective actions. As a result, considerable human interaction is necessary to perform dynamic studies and also to interpret the results.

However, since the last two decades, power systems have suffered many changes, highlighted by the open access to competitive electricity markets and by the large integration of variable renewable energies sources, leading power systems into a highly unpredictable operating scenario and thereby the conventional off-line dynamic security analysis practice became inadequate and non-economical [13]. Therefore, a growing need to move dynamic security assessment to real-time has been verified. As a result, the continuous monitoring of system's dynamic security conditions could be performed in order to reduce the risk of dynamic insecurity and the possibility of system's collapse, by including on-line dynamic security assessment capacity in the modern energy management systems.

As a promising alternative, intelligent systems based on automatic learning techniques have shown encouraging application potential to fast dynamic security assessment [14], by providing a

fast analysis for transient stability studies and reducing the mathematical complexity. Therefore, the initial idea of using pattern recognition for security assessment dates back to 1968 [90]. Pattern recognition is characterized for its ability to "learn" the process behavior from the data relationship between inputs and outputs, without any prior understanding of the process behavior and no phenomenological understanding of the process itself [90]. Additionally, ANNs have been shown to work well for this application [88]. A more detailed approach is addressed in chapter 4 concerning ANNs. Moreover, the first systematic investigation of automatic learning techniques, such as Decision Trees, to this area was performed in the late 80s [88]. Since then, various advanced automatic learning techniques as well as data mining and machine learning approaches have been used to the development of fast dynamic security assessment and acceptable results have been achieved. By directly capturing the relationship between system parameters (inputs) and the dynamic security status (outputs) from a database, the dynamic security analysis can be accomplished by automatic learning techniques and extract the additional useful knowledge for dynamic security analysis (e.g. preventive and corrective controls actions) [13]. Additionally, automatic learning techniques can also extract useful knowledge from system dynamic security characteristics which can be used for security controls, facilitating real-time dynamic security assessment in practice. Generally, the development of the automatic learning techniques for dynamic security analysis consists of four stages, as follows:
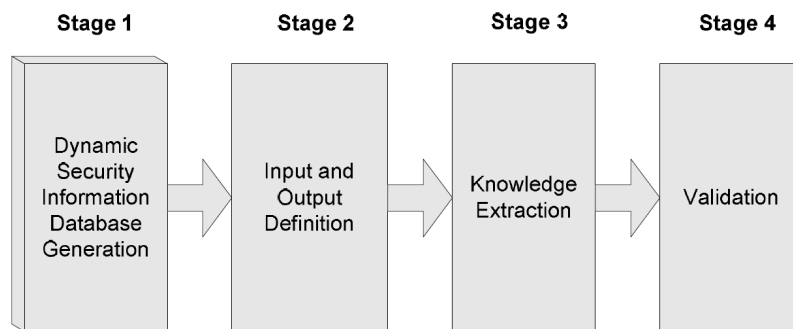
Figure 2.15: Stages to develop automatic learning techniques for dynamic security analysis [13]

First, a database that contains system dynamic security information is generated. Such a database should be accurate and able to match practical operating conditions, which needs to be evaluated. Second, the inputs and the outputs are defined, i.e. which system parameters should be used to evaluate the system security, and how the security is characterized. Then, the knowledge is extracted from the database and is reformulated for on-line application purpose. Finally, the validation stage is performed to evaluate the accuracy and robustness of the process. If necessary, some corrections are needed if the automatic learning technique is shown insufficiently good. For each stage, especially for the second and the third stages, there are different techniques and algorithms that can be adopted, which can result in different dynamic security assessment models.

Automatic learning techniques, which are the foundations of intelligent systems for dynamic security analysis, can also be used to define the best control actions to be taken based on the

security conditions, as mentioned before. The structure of such a system is shown in figure 2.16. The system measurements that can be obtained from a number of sources (the traditional SCADA systems, PMUs and disturbance monitors) are fed directly into the intelligent system that has access to both knowledge base as well as deterministic tools.
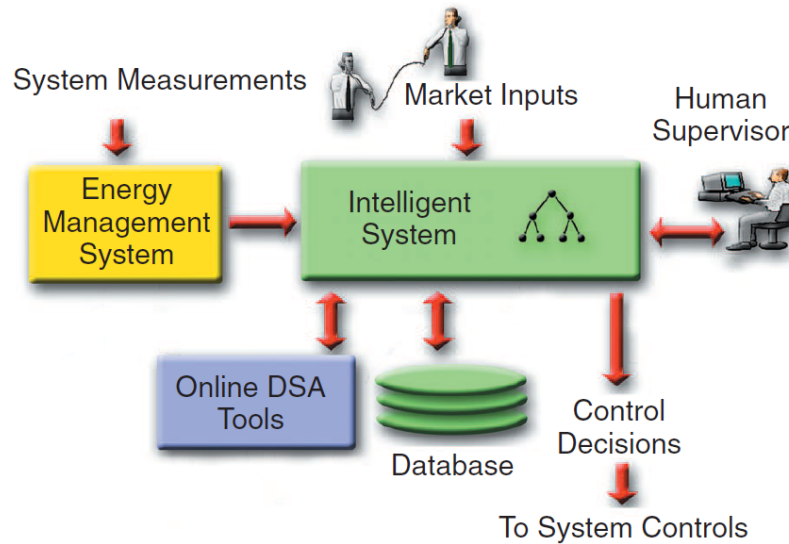

Figure 2.16: Architecture of a dynamic security assessment system [14]

These intelligent systems interact with dynamic security simulation tools and a knowledge database. If the intelligent systems can determine the security condition, then the results are provided immediately. Otherwise simulations are performed and the results provided to the operator and the knowledge database is updated accordingly [14].

As a result, on-line dynamic security assessment can provide the first defence against widespread system disturbances and failures by quickly and accurately scanning the system for potential problems and providing to system operators actionable results. With the development of emerging technologies concerning intelligent systems based on automatic learning techniques, on-line dynamic security assessment is expected to become a dominant tool against system collapse [14].

2.7 Summary

In this chapter, a general overview and literature analysis about the paradigm change in power systems that results from high levels of RES penetration in isolated power systems is presented.

The increase of renewable energy units in electrical power systems has been promoted worldwide as a mean of reducing energy costs, CO_2 emissions and coal and oil dependence. This increase has been possible not only because of the establishment of new targets and the change in energy policies but also because of the technical maturity and steady cost declining that some solutions such as wind and PV energy conversion have reached over the last years.

Simultaneously, quality of service and security criteria have become more stringent and therefore, voltage and frequency operation limits have been the subject of concern and monitoring by the TSOs. Due to the mechanical and electrical coupling of SGs with grid and thus the capacity that this type of machines has for inherently contribute with synchronous inertia to the system makes SGs very important for frequency and system stability.

However, PV units and wind turbines are types of converter-interfaced generators, and thus, no mechanical and electrical coupling with the grid is achieved. This type of power generation is not capable of working in synchronism with grid and cannot contribute to the overall synchronous inertia of the system, which is essential to keep frequency within the acceptable limits and counteract possible frequency deviations during a disturbance. Another important aspect is the fact that the amount of inertia present in power systems will become dependent on the generation mix dispatched for a particular time, affected by the wind and solar conditions. Additionally, due to the reduced number of conventional generators in power systems of smaller dimensions, the resultant effects by the deployment of this type of machines by non-SGs will be more severe than in bigger and well-interconnected power systems, as a result of low inertia levels.

Therefore, the literature analysis performed in this chapter allows concluding that wind and PV power plants must be capable of providing voltage and frequency support and new grid codes must be developed by grid operators in order to increase RES share in power systems.

Many frequency control techniques have been proposed, and the majority of them are based on the concept that CIG should mimic synchronous machines response when an under-frequency event occurs. As a result, CIG must have a power margin to be released during a disturbance. For that purpose, deloanding techniques were studied over the last years for wind turbines and PV panels in order to guarantee such power margin. Additionally, ESS like batteries, flywheels and supercapacitors have been used, especially with PV systems, so that a sufficient margin could be guaranteed. Consequently, many additional control loops and controllers have been developed to force non-SGs to respond to power variations by releasing the extra power, such as droop controls, inertia emulation techniques and fast power reserve.

However, some of these controllers are subject to noise, delays and possible instabilities, especially those who based their actuation in frequency measurements. Therefore, more research is needed to overcome controllers limitations and more methodologies has to be defined to evaluate the required synchronous inertia to maintain systems stability and to make possible a future 100% renewable energy based power systems scenario.

Chapter 3

Methodology and Dynamic Model in MATLAB/SIMULINK

3.1 Introduction

In this chapter, the methodology adopted as well as the dynamic model of the power system developed in a MATLAB/SIMULINK platform, which served as the simulation framework for the developments of this thesis, will be presented in detail. This model was used in order to study system frequency response for two different contingencies: loss of 50% of the active power output from wind and PV plants and loss of the biggest thermal unit in the system. A comprehensive description of each constituent model is performed in this chapter, specifically the thermal diesel and hydraulic generator units models. Additionally, a MATLAB's script was developed to define all the necessary parameters to be sent to the SIMULINK model. The complete model layout can be found in appendix A.

3.2 Methodology

This section aims to present the methodology adopted for the development of this thesis. Such methodology is based on three main steps, they are:

1. Identification of possible operation scenarios of load and generation

2. System dynamic behavior study and functional data set generation using a MATLAB/SIMULINK platform

3. Utilization of ANN trained to emulate the dynamic response of the system under analysis for the pre-specified disturbances

In order to achieve the first step, it was considered a suitable power system used as a case study. This system is characterized for its small dimension and by a non-negligible wind and PV energy penetration, so that a large number of operation scenarios could have its demand guaranteed

mainly by wind and PV sources. A more detailed description of this power system is presented in section 3.4.1. By considering such power system, it is important to study all the technically feasible operation points that are going to be subject to an active power dispatch. This dispatch is subject to certain constraints, which are mentioned in section 3.4.2.

After the operation points and its dispatch have been created, they were used as inputs for the MATLAB/SIMULINK model in order to study the power system dynamic behavior when subjected to two different disturbances, section 3.5. The dynamic behavior evaluation is based in two measurements (MATLAB/SIMULINK model outputs), they are: frequency nadir (Hz) and the RoCoF (RoCoF) (Hz/s). Additionally, it was considered the presence of SCs in the system so that its influence in system behavior could be analysed and more operation points could be generated. Moreover, this platform not only allows to perform dynamic studies but also to create the data set useful to the ANN training process, which leads to the third main step of this thesis framework.

The use of ANN in this thesis aims to emulate, in a fast manner, frequency response from the system for a certain operation scenario, and specifically be able to present a frequency nadir and RoCoF values as close as possible to the ones obtained in MATLAB/SIMULINK simulations. For that purpose, two different ANN were created, one ANN for each disturbance, and its performance was evaluated through its RMSE (Root Mean Square Error) value. With the two ANN trained, a sensitivity analysis took place so that the minimum synchronous inertia to improve dynamic security in the power system could be obtained for all the considered operation scenarios. The framework for such sensibility analysis is explained in detail in chapter 4.

3.3 Dynamic Models

This section deals with the modelling of power system machines in MATLAB/SIMULINK as well as the options and the assumptions adopted for the dynamic studies of the system in this software for two different contingencies and considering (or not) the presence of SCs in the system. Additionally, this dynamic system model is based on a single bus and only considers speed regulation for frequency control purposes, neglecting the electrical behavior of the electric machines and their voltage control loops, which turns this model into a not complete and detailed model. Moreover, wind and solar power plants were modelled as power injectors without participation on frequency control.

3.3.1 Thermal Generator Unit

Thermal power units are, as mentioned in previous sections, a type of conventional synchronous machines that can be modeled through its frequency control functions. Therefore, its swing equation can be modeled as follows:
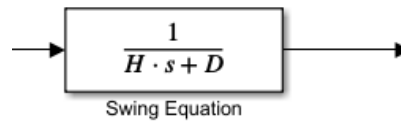
Figure 3.1: Swing equation transfer function

Where M is the machine inertia constant in seconds (s) and D is the load-damping constant in (p.u.MW/rad/s).

The thermal speed governor can be represented as follows:
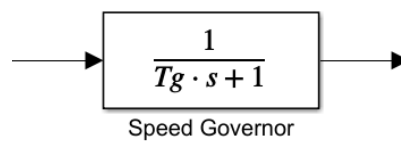
Figure 3.2: Thermal speed governor transfer function

Where T_g is the speed governor time constant in seconds (s).

Additionally, the thermal turbine can be modeled as follows:
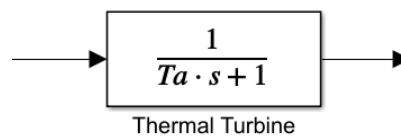
Figure 3.3: Thermal turbine transfer function

Where T_a is the thermal unit time constant in seconds (s).

Figure 3.4 presents an open loop system. The system is described by the speed governor, turbine and the generator that allows studying the variation of the frequency (Df(s)) depending on the load (DPL(s)).
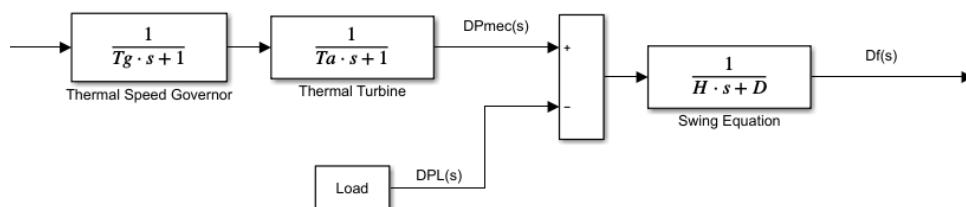
Figure 3.4: Open loop system

Therefore, as mentioned in the previous section, applying a load variation will lead to frequency deviations. However, in power systems, large frequency deviations are not acceptable, and for that reason, it is necessary to implement a control system. One of the simplest methodologies

is to create a closed loop with a proportional control. This loop allows doing a primary control relating the frequency and power by expression 3.1.

$$R = \frac{\Delta f}{\Delta P} \tag{3.1}$$

Where R, (p.u. Hz/p.u. MW) represents the ratio of speed deviation (Δf) to change in power output (ΔP). It can also be mentioned as the machine's droop.
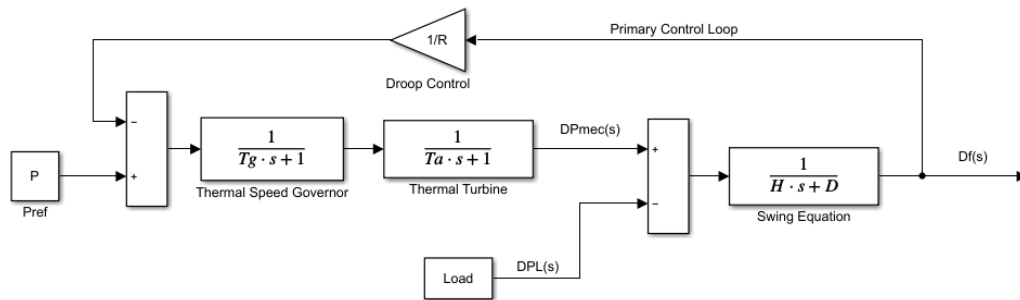
Figure 3.5: Thermal unit primary control loop

The control loop has a proportional gain (1/R) that amplifies the speed error and this way the turbine valve position is controlled, contributing to contain frequency deviation. In order to bring the system frequency to its nominal value and therefore, eliminating the remaining error, a secondary control loop (or integral control loop) is added, as shown in figure 3.6:
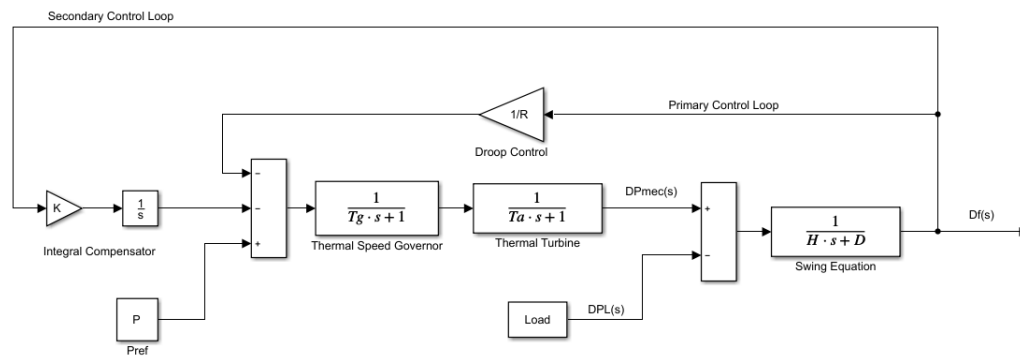
Figure 3.6: Thermal unit primary and secondary control loop

Where k is the secondary control integral gain.

The rotor speed is measured and compared with the speed reference, and the resulting error is amplified and integrated in order to become a control signal useful to regulate the turbine valve position and as a result, to control the generator active power output.

3.3.2 Hydro Generator Unit

The simulation model of a Hydraulic unit, figure 3.7, is very similar to the Thermal unit model. Both generating units have primary and secondary control loops, but the hydraulic turbine has transient droop compensation. Such transient droop compensation exists due to the hydraulic turbine's power response to a change in its valves and represents the time delay due to water inertia starting time. Therefore, a change in valves position for a larger or smaller amount in mechanical power has an opposite effect in the initial turbine power, as shown in figure 3.8. Due to the water inertia, the water pressure during the opening of the valves is low, and the mechanical power will drop. Contrary, after a few seconds, an overshoot in mechanical power take place because the valves closing process causes an increase in water pressure. Therefore, this transient compensation aims to retard the speed error amplification, so that the water inertia phenomena could be compensated.

Figure 3.7: Hydro unit primary and secondary control loop

Where T_r is the reset time in seconds (s), r is the transient droop (p.u. Hz/p.u. MW) and T_w is the water starting time in seconds (s).
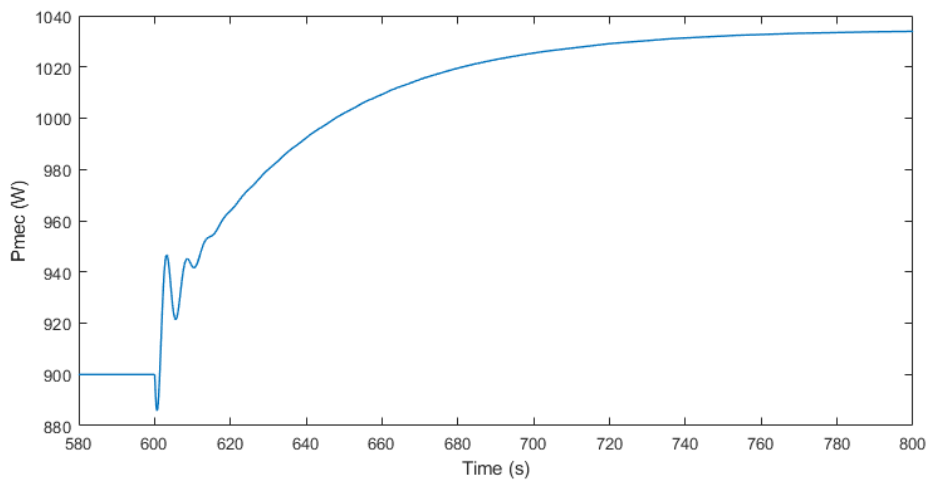
Figure 3.8: Hydro turbine power characteristic response

3.3.3   Wind and PV Farm

The wind and PV farms present in the power system used for the development of this work are only modelling as an active power injector, thereby contributing with a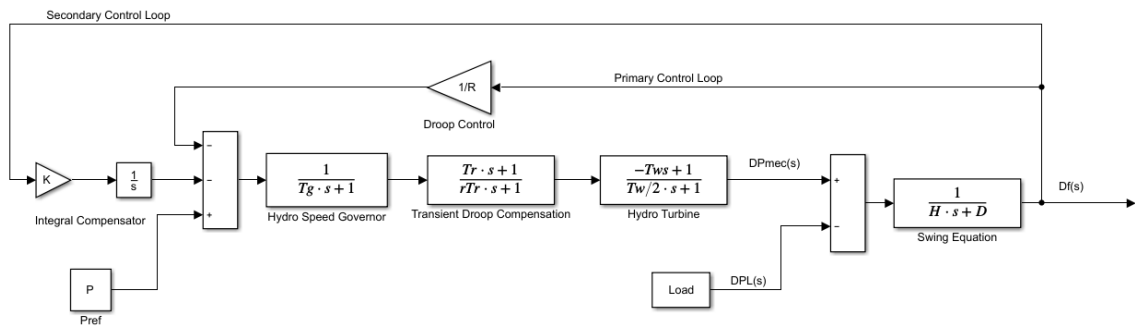ctive power for load satisfaction only. Therefore, and because wind and PV sources are connected to the grid through power electronic devices, no inertia and frequency regulation can be provided by wind and PV farms to the power system.

In the MATLAB/SIMULINK platform, both wind and PV farms were modelling through the use of a *Signal Builder* block followed by a *Gain* block, as shown in figures 3.9 and 3.10.
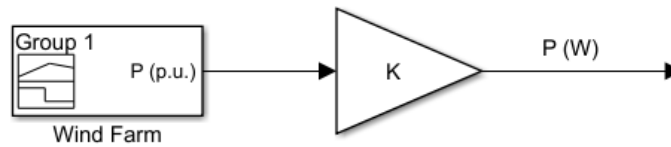
Figure 3.9: Wind farm simulation model
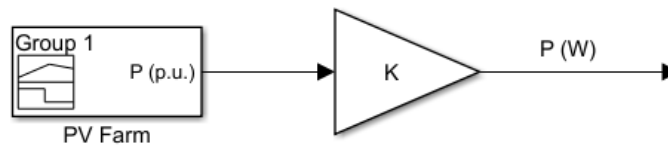
Figure 3.10: PV farm simulation model

The *Signal Builder* block was used to easily represent the disturbance, namely the loss of 50% of active power output from wind and PV plants. However, because the *Signal Builder* power output is in p.u., it must be multiplied by its active power output in watts. The disturbance representation is presented in section 3.5.1.

As a result, the complete and detailed power system's models developed and performed in MATLAB/SIMULINK can be found in appendix A.

3.4   Power System and Dispatch

This section aims to present the power system used as a case study for the development of this thesis. It is important to refer that the power system used does not exist. However, it can be representative of many islanded power systems. For the purpose of this thesis, it was considered a non-negligible presence of renewable energy sources (wind and PV energy) into the generation mix in order to evaluate its technical impacts on the system. In this section, it is also shown the framework used to generate all the feasible active power dispatch results, which will be used as operation points (inputs) for the dynamic simulation to be executed in MATLAB/SIMULINK platform.

3.4.1 Power System Description

In table 3.1, it is presented the power system generation mix consisting of five thermal units, two hydro power plants, one wind farm and one solar farm. The active power output limits and nominal active power are also presented.

Table 3.1: Power System Generation Mix

Generation Unit	P_N [kW]	P_{max} [kW]	P_{min} [kW]
Thermal 1	2640	2520	1200
Thermal 2	2320	2200	1080
Thermal 3	2520	2400	1120
Thermal 4	2420	2300	1180
Thermal 5	2280	2160	1000
Hydro 1	2120	2000	1000
Hydro 2	1920	1800	880
Wind Farm	4350	4000	0
PV Farm	660	600	0
Total [kW]	21230	19980	7460

Additionally, in table 3.2, it is shown the inertia constant of thermal and hydro SGs present in the system with a constant of inertia of 3 and 2 seconds, respectively.

Table 3.2: Thermal and Hydro machines constant of inertia [H]

Machine	Inertia Constant [H]
Thermal Units	3 (s)
Hydro Units	2 (s)

In figure 3.11, it is shown the single bus power system's diagram with all the generation units as well as the load. The detailed model developed in MATLAB/SIMULINK can be consulted in figures A.1 and A.2, present in appendix A.
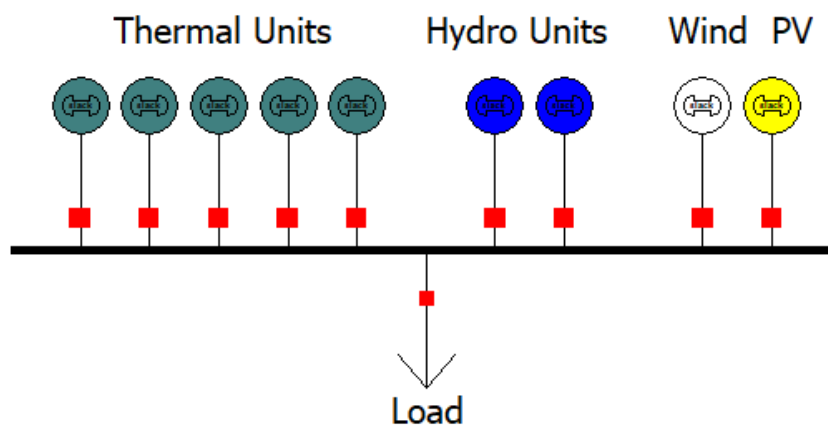
Figure 3.11: Single bus power system's diagram

In figure 3.12, it is shown the percentage of conventional (thermal and hydro) active power installed capacity and the wind and solar active power installed capacity. As shown in figure 3.12, 24% of the total active power installed capacity is provided by non-conventional power plants (wind and solar), which shows that the system under study has a high level of renewable integration as desired.
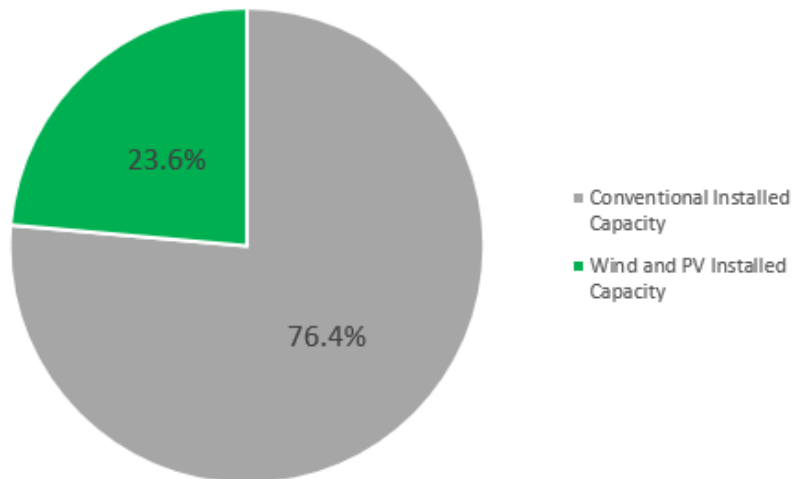
Figure 3.12: Conventional and wind and PV active power installed capacity percentage.

Additionally, in figure 3.13, it is presented the percentage of the active power capacity of each type of energy source in the power system.
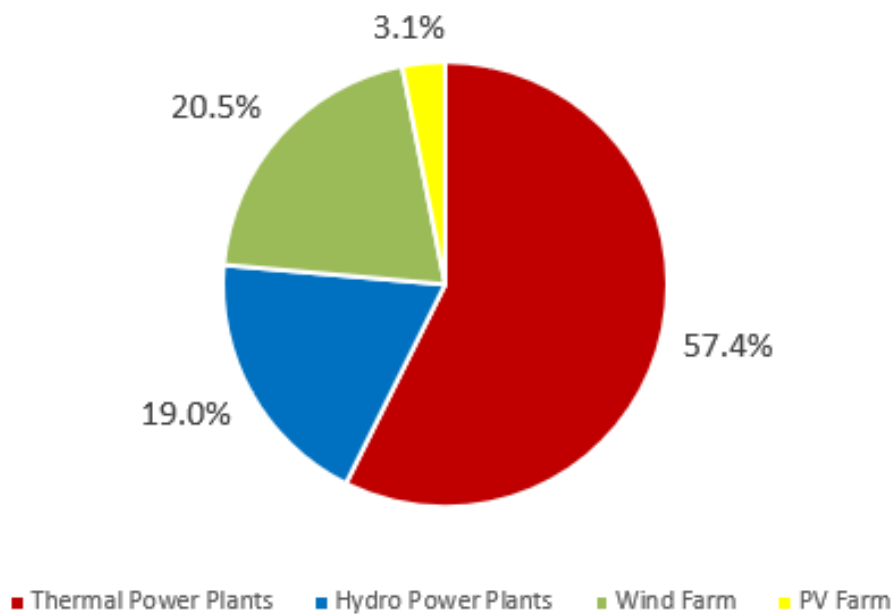
Figure 3.13: Active power installed capacity by type of energy source.

3.4.2 Dispatch and Operation Points Generation

The following subsection presents the methodology adopted so that all the operation scenarios could be generated and thus a power dispatch could be applied over those operating points for dynamic studies purpose in MATLAB/SIMULINK.

As a result, the following constraints must be considered:

- The active power output limits of the machines;

- At least one thermal unit in operation for each operation scenario;

- Having in mind the need to include a security criteria, it must be ensured that the spinning reserve is equal or bigger than the nominal active power of the biggest machine (thermal unit $n^o 1$);

Hereupon, it was possible to create 38376 different possible operation points for the system, by varying the load between 2,9 MW and 10 MW with steps of 100 kW and varying the wind production between 0 and 4 MW with steps of 100 kW and varying solar production between 0 and 600 kW with steps of 50 kW. Therefore, these 38376 operation points were subjected to an active power dispatch by thermal and hydro units. For that purpose, an unit-commitment strategy was followed, based in a merit order where solar and wind sources were considered the cheapest generation units and thermal units the most expensive sources. The operation costs of each machine can be represented in a simplified manner as follows:

$$C_i (P_{Gi}) = P_{Gi} \times k_i \tag{3.2}$$

Where $C_i (P_{Gi})$ is the operation costs of machine i as function of its active power production, P_{Gi}. k_i is the constant used as a penalty.

The following table 3.3 presents the constant k for the different types of power sources in the system.

Table 3.3: Constant k for all the generation units

Generation Unit	k
Thermal Units	10000000
Hydro Units	100000
Wind Farm	1000
PV Farm	10

By adopting this approach, it is possible to guarantee that wind and solar power plants are a priority in the dispatch and therefore, having a more significant participation in power supply for each operation point.

The dispatch was calculated so that the active power output of each machine in the system could be known for all the 38376 points. However, it is important to mention that some of the operating points have lead to the same dispatch result due to machine power limits and due to the

constraints already mentioned. Therefore, in these cases, they were not considered as inputs for the neural networks training process, as explained in chapter 4.

In order to easily understand wind and solar penetration levels achieved for the total operation points generated, in figure 3.14 it is presented the different wind and solar penetration levels and its frequency considering all the 38376 operation points. Thus, the most common wind and PV penetration levels range from 10% to almost 45% with a frequency between 9,5% and 11% of the total operation points. Therefore, this figure shows that there are a large number of scenarios where wind and PV production are considerably high, as desired.
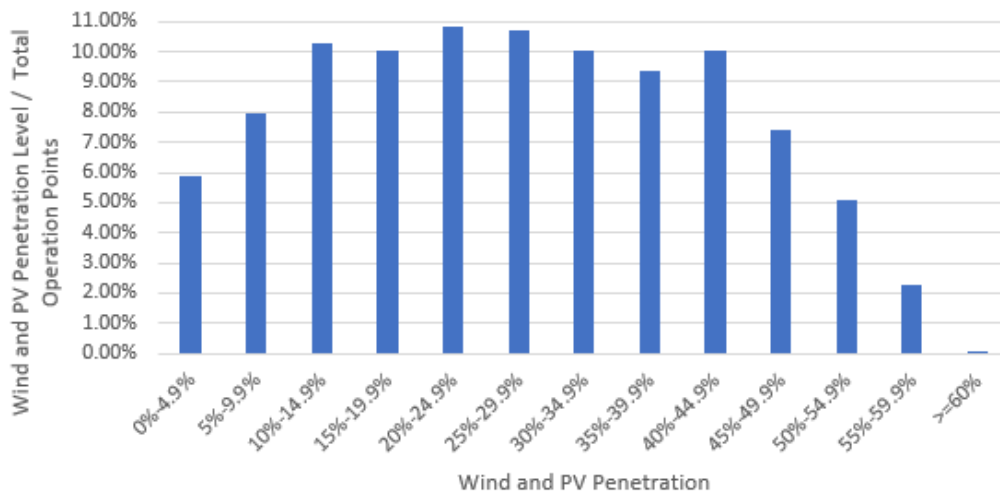
Figure 3.14: Wind and PV penetration level frequency

3.5   Disturbances

In this section, the different disturbances studied during the development of this thesis are presented. As mentioned previously, these disturbances are a mean to study system dynamic behavior and they also play an important role in the data set generation to be used during the ANN training process and that will result in a functional knowledge database. During the dynamic simulations in MATLAB/SIMULINK, the dynamic response of the system was evaluated through the measurements of frequency nadir (Hz) and the RoCoF (Hz/s) and checked if they were within the established limits. Such limits are: a minimum limit of 47.5 Hz for frequency nadir and a maximum limit of 2 Hz/s for the RoCoF value. Therefore, after the contingency occurs, if the system has the capacity not to suffer a frequency deviation greater than 2.5 Hz or a RoCoF bigger than 2 Hz/s (the green region in figure 3.15), it can be considered stable.
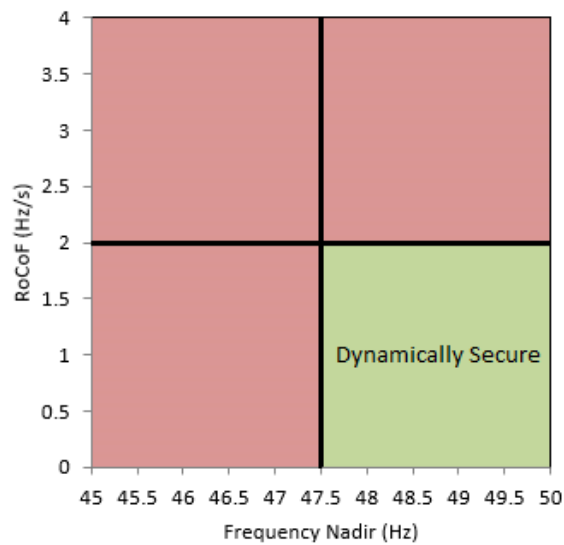
Figure 3.15: Security domain representation

3.5.1 Loss of 50% of Wind and PV Active Power Output

Accordingly to the power system generation mix and the dispatch results, non-conventional energy sources have a considerable high contribution to feed the load in the majority of the operation points generated, as shown in figure 3.14. Therefore, because of wind and solar penetration levels are non-negligible and these power sources rely on the availability of wind and solar resources, it is very important to study system's dynamic response when an outage of wind and solar power production occurs. In this work, a sudden loss of half of the wind and solar production is considered. When such disturbance occurs, the main concern is to respect the security criteria that assures the avoidance of automatic load curtailment. Figure 3.16 shows the disturbance modelling in MATLAB/SIMULINK through *Signal Builder* blocks.
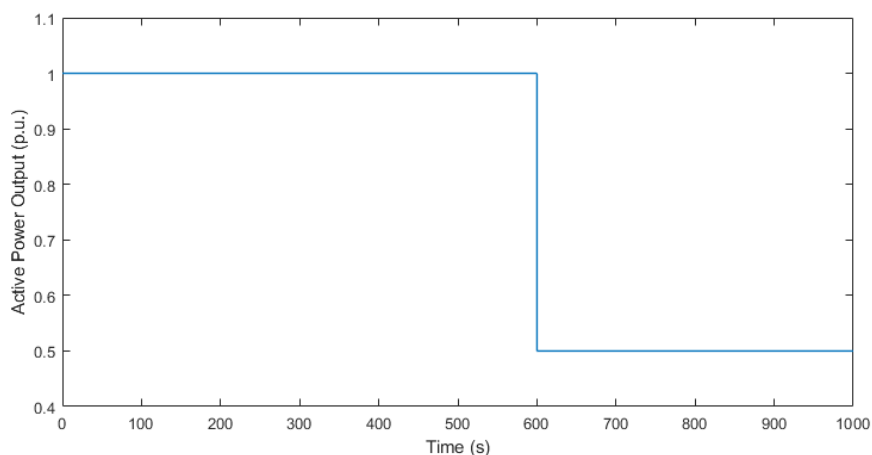
Figure 3.16: Contingency 1: wind and PV active power loss

3.5.2   Loss of the Biggest Thermal Unit

The thermal unit 1 tripping is the second contingency to be performed in the simulation platform for dynamic studies purpose. This type of disturbance can occur in many power systems, and because thermal unit 1 is the biggest machine in the power system, such disturbance can have a major impact in the system's dynamic security. Figure 3.17 shows how this disturbance was modelled in MATLAB/SIMULINK.
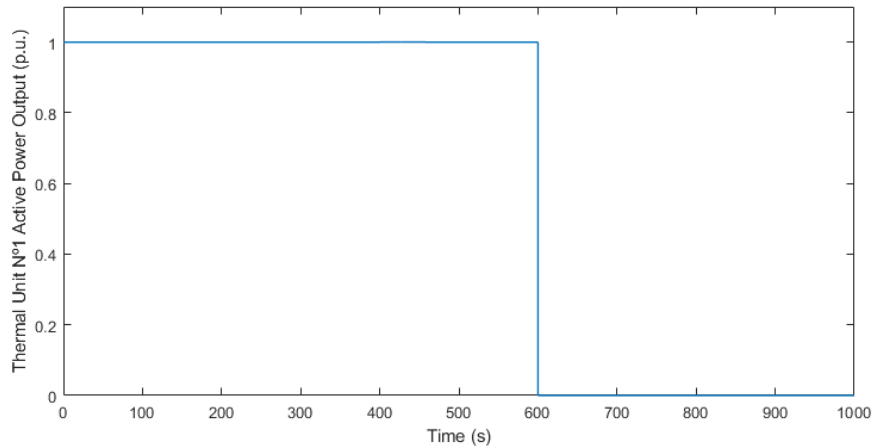
Figure 3.17: Contingency 2: thermal unit 1 tripping

3.6   Summary

This third chapter aimed to expose the methodology adopted to achieve the goals of this thesis as well as to demonstrate and explain the power system modelling developed in MATLAB/SIMULINK simulation platform. It was also the purpose of this chapter to present a general description of the power system used as a case study, where wind and PV sources are responsible for almost 24% of the system active power installed capacity, and to expose the methodology used to generate all the operation points considered in this work as well as its power dispatch calculation. It was generated and simulated 38376 operation points.

The power system dynamic model developed is based on a single bus model where only machine's frequency control loops are modeled. Additionally, wind and PV farms are modeled by an active power injector model and, therefore, they do not participate in frequency regulation. A brief overview about the disturbances simulated is also exploited in this chapter.

Chapter 4

Artificial Neural Network

4.1 Introduction

The dynamic analysis of a power system after a disturbance is a very time demanding task. Thus in recent years, a large effort has been made toward developing fast approaches to deal with the prediction of system dynamic behavior, using namely ANNs. In this chapter, it is presented the framework used to develop two ANNs to emulate the systems dynamic frequency response when facing a certain disturbance through the motivation of trying to provide a fast system security assessment and the identification of effective control measures that prevent systems collapse by performing an ANNs sensibility analysis.

Therefore, in section 4.2, some backgrounds concerning the use of automatic learning techniques, such as ANN, for fast dynamic security assessment are presented. In section 4.3 the steps taken to design the proposed ANNs will be addressed, namely: feature selection and data set generation, followed by an ANN sensibility analysis useful to develop a preventive control strategy by identifying the minimum synchronous inertia required to maintain system security, in subsection 4.3.4.

4.2 Backgrounds

In islanded power systems, some technical constraints are limiting RES integration due to dynamic security problems that may arise in certain conditions. In fact, islanded power systems, when compared with well-interconnected power systems, are less robust due to the low inertia time constants and to the nonexistence of interconnection with neighboring systems that help reducing reserve requirements. Isolated power systems with significant wind and solar power integration are exposed to sudden wind speed and radiation variations. Therefore, wind generation tripping or wind power variations, as well as solar power variations in islanded power systems, need to be quickly compensated by thermal units in order to avoid large frequency excursions that may lead to system collapse. In fact, a fault occurring in an isolated system may cause cascading events leading to system collapse: frequency deviation may lead to the activation of under frequency

load tripping of generation groups. In order to face severe contingencies, system operators usually follow very restrictive policies in terms of spinning reserve requirements, which may lead to the under-exploitation of wind power generation capabilities.

The most critical issue when evaluating system security in isolated power systems is the system frequency deviation and the RoCoF following a pre-defining disturbance. Therefore, minimum frequency deviation and RoCoF are the natural security indexes used for dynamic security assessment in islanded power systems. Automatic learning techniques such as ANN has been used so that the security assessment framework could be developed [91]. These techniques are based on the exploitation of a large data set containing information about power system dynamic behavior - the functional knowledge database - for a large number of feasible operating scenarios. The data set is generated, as mentioned in the previous chapter, through the use of the dynamic simulation platforms described before. The use of ANNs for dynamic behavior assessment define the security evaluation tool that can be used for the continuous monitoring of system security and be responsible for presenting to system operators adequate preventive control actions, namely the use of SCs, redispatching power units production or determining secure unit commitment alternatives for the coming hours, in case of detection of insecure scenarios.

The need to achieve not only fast accurate measures of the transient stability degree but also an easy way to determine preventive control measures led to the adoption of ANNs. The application of ANNs for dynamic security evaluation was previously used by Sobajic and Pao [92] for fast assessment of critical clearing time. Kumar et al. [93] described in a general way the requirements needed by ANNs to evaluate dynamic security in large power systems. Djukanovic et al. [94] presented a new ANN approach for the determination of load shedding amount so that transient stability could be assured. The on-line management of preventive control mechanisms requires knowledge about the power system dynamic behavior for each specific scenario. The traditional and most accurate analysis of this kind of problems involves the numerical solution of non-linear equations, requiring the use of simulation platforms, which is a very demanding and time consuming computational task and it is not suitable for fast assessment purposes. Therefore, automatic learning techniques based tools are an alternative approach since they provide effective means of extracting high-level knowledge from large data sets in order to help on-line system management and operation regarding these dynamic issues. The referred data sets should contain detailed information about the power system dynamic behavior. This information should be generated off-line by making use of appropriated simulation platforms. In order to perform a fast dynamic security assessment of an islanded power system, it is necessary to develop a tool able to emulate the system dynamic behavior and the synchronous inertia required to be added in the system to keep it stable.

Therefore, ANNs are an essential piece of the methodology developed within this thesis. Not only do they perform better than traditional statistical methods in the dynamic security pattern classification [95], but they also provide means for evaluating the degree of security. Moreover, they provide simple and effective ways of computing the derivatives of a security index with respect to the control variables. Such ability allows the application of gradient-based methods

which allows moving an insecure state into the dynamic security domain.

4.3 Security Assessment Using ANN

The on-line power system management and its fast dynamic security assessment require knowledge about its dynamic behavior following a disturbance. In order to emulate the dynamic behavior and to evaluate the synchronous inertia required to be present in the system to move it into the dynamic security domain, it is necessary to develop an intelligent system able to predict the synchronous inertia as a function of pre-disturbance variables that are able to characterize the system operating scenario. It is well known that ANN can be easily exploited in order to perform regressions over a set of input-output pairs. The development of a tool in order to deal with the referred dynamic issues involves the following steps:

- Generation of a large data set containing information of power system dynamic behavior for the selected disturbances (biggest thermal unit tripping and loss of 50% of wind and PV production) - the functional knowledge database;

- Training and performance evaluation of the ANN architecture in order to accurately emulate system dynamic behavior in terms of RoCoF and frequency nadir for the pre-defining contingencies;

- Exploiting the ANN tool for the on-line identification of preventive control actions in order to increase the dynamic security;

These three steps will be under analysis in the following sections of this chapter.

4.3.1 ANN Architecture

In this thesis, the Neural Fitting app called *nftool* from MATLAB was used to define the ANNs architecture and to train them. It was used a two-layer feed-forward ANNs with sigmoid hidden neurons and linear output neurons. The ANN training process will be achieved through the Levenberg-Marquardt backpropagation algorithm.

4.3.1.1 Feature Selection

The feature selection process needs a special attention. A pre-identification of the relevant variables that are going to characterize a given operation scenario is an important step for a successful application of these techniques. Sometimes a pre-processing stage is needed to select the most relevant variables to be used as inputs of an ANN. However, in this work, it was just selected a set of meaningful variables considering some aspects: each operating point generated is characterized by a set of system measurements that could be used as ANNs inputs. The input data should appropriately characterize the system state, but at the same time, the input set should be as small as

possible to avoid a large number of ANN input variables while still having enough discriminating ability. In this work, the following set of system explicative variables were used as inputs:

- Generated active power outputs (from thermal, hydro, wind and solar units);

- Spinning Reserve;

- Total machines inertia constant (in operation);

- Total SCs inertia constant;

For fast security assessment purpose by ANNs, it is important that input variables are independent and controllable, allowing to control the effects in ANN output from any change in the input variables. Considering the selected input variables, the only independent variable is the total SCs inertia constant. Thus it was used as a control variable in ANNs sensitivity analysis.

It is shown, in figure 4.1, the architecture of both ANNs developed in this work where it is possible to verify all the inputs mentioned before and the natural outputs, RoCoF and frequency nadir, as result of frequency response emulation by the ANNs.
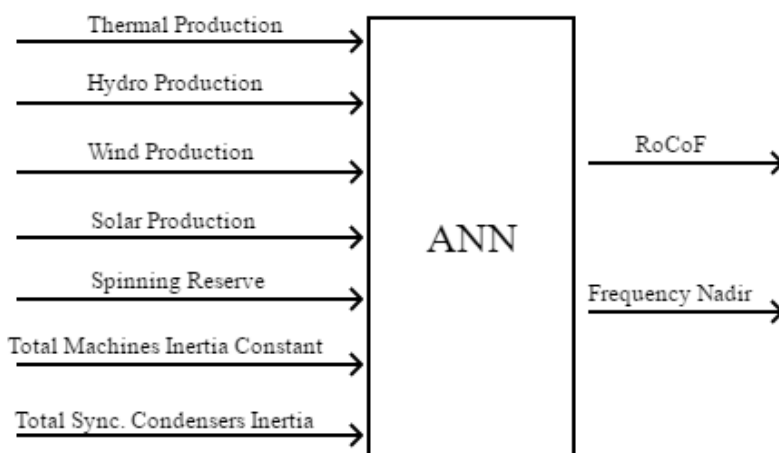
Figure 4.1: ANN architecture

The ANNs architecture consists of 12 input units, 30 hidden neurons and 2 outputs. This architecture has led to the best performance results, as shown in table 4.1.

4.3.2 Data Set Generation

Power system dynamic behavior in the moments after a disturbance is highly dependent on the power system load and generation profile and the disturbance itself. Therefore, the data set to be generated should cover a large number of different operating scenarios of load and generation. As mentioned in section 3.4.2, the data set has been generated by the MATLAB/SIMULINK simulation platform by varying the total load, the wind active power and the solar active power. This

data set comprised 153504 patterns (38376 patterns for each additional SCs inertia constant of 0s, 2s, 3s and 5s). However, some of these points have the same dispatch result due the constraints already mentioned in 3.4.2 and, therefore, they must be eliminated from the data set so that all the operation points could be different ANNs inputs, improving the training process. As a result, from these 153504 patterns, only 102968 were considered. For the training process, 68646 (two-thirds) were used and 34322 (one-third) for the testing purpose were used. Each operating point is characterized by a RoCoF and frequency nadir value, obtained from a complete dynamic simulation performed for several seconds after wind and solar perturbation or a thermal unit tripping defined according to figures 3.16 and 3.17. These variables have been chosen as the ANN outputs. Additionally, it is important to notice that generated active power and spinning reserve inputs were subjected to a decimal normalization and frequency nadir output was normalized in the interval [0, 1] so that better ANN performance could be achieved.

Moreover, due to the potentially numerous system disturbances, it is unfeasible to create an ANN that could predict the systems dynamic behavior for all of them. Therefore, it was developed an approach so that a single ANN could be used to deal with a single pre-defined disturbance properly.

4.3.3 ANN Performance

After the training process, the architecture with the lowest root mean square error (RMSE), equation 4.1, in all data set for each contingency is presented in table 4.1. It is important to notice that contingency 1 concerns to loss of wind and PV power output and contingency 2 regard thermal unit 1 tripping.

$$RMSE = \sqrt{\frac{1}{N}\sum_{i=1}^{N}(y_i - \widehat{y_i})^2}$$

(4.1)

Where $\widehat{y_i}$ is the predicted value.

Table 4.1: ANNs performance

Contingency	Nr. Train Patterns	Nr. Test Patterns	ANN Topology	RMSE (RoCoF)	RMSE (Frequency Nadir)
1	68646	34322	12-30-2	0.000333	0.003631
2	68646	34322	12-30-2	0.000043	0.000603

For both contingencies, the architecture with the lowest root mean square error has been (12-30-2): 12 input units, 30 hidden neurons and 2 outputs.

The numerical results obtained from the dynamic simulator and the ANN for one operation point used as an example can be seen numerically in table 4.2. As expected, the ANN provides results that match quite well in comparison with the ones obtained from full dynamic simulation given through MATLAB/SIMULINK.

Table 4.2: Dynamic Simulation versus ANN

	Contingency 1			Contingency 2		
	Dynamic Simulation	ANN	Abs. Difference	Dynamic Simulation	ANN	Abs. Difference
Frequency Nadir (Hz)	46.78453	46.78625	0.00172	46.79839	46.79828	0.00011
RoCoF (Hz/s)	3.21802	3.21809	0.00007	3.95646	3.95645	0.00001

4.3.4 Preventive Control Actions

As the ANN emulates the dynamic behavior of the power system, preventive control actions are required when dynamic insecure operating points are detected. This should be developed by identifying the values of the control variables (input variables) that satisfy the constraints in 4.3 and 4.4. For this preventive control strategy only changes in total SCs inertia constant values was allowed, corresponding to the addition of more synchronous inertia into the system. Total SCs inertia constant is the only independent ANN's input variable and for that reason this controllable variable was selected to perform the sensitivity analysis, preventing the use of a chain rule which would make all the process very demanding and time consuming. Therefore, the general problem can be formalized as a typical optimization problem:

$$min(H_{ad}) \tag{4.2}$$

Subject to:

$$RoCoF < 2 \ (Hz/s) \tag{4.3}$$

$$FreqMin > 47.5 \ (Hz) \tag{4.4}$$

Where the objective function minimizes the amount of additional synchronous inertia to be added to the system so that constrains 4.3 and 4.4 could be satisfied.

Determining the minimum amount of synchronous inertia to be added to the system can be easily performed through a gradient search technique. ANN provides a simple and efficient way to evaluate the sensitivities of the output relative to the input variables. In this case study, this is achieved by computing numerically the derivatives of the RoCoF and frequency nadir with respect to the chosen control variable, which is the total SCs inertia constant, as follows:

$$\frac{\partial RoCoF}{\partial H_{sc}} \tag{4.5}$$

$$\frac{\partial FreqNadir}{\partial H_{sc}} \tag{4.6}$$

where

H_{sc} is the control variable

FreqNadir is the frequency nadir output

Defining preventive control actions requires for each operating point:

- accuracy evaluation of RoCoF and frequency nadir, using the designed ANNs;

- if RoCoF>2(Hz/s) or frequency nadir<47.5(Hz) (unsafe operation point), some changes in the control variable are required in order to decrease RoCoF value and increase frequency nadir value, moving the system towards its dynamic security domain; this job is performed by an algorithm developed on a MATLAB's script for the purpose of this thesis;

The following algorithm searches, for each detected insecure operation scenario, the minimum amount of inertia that must be added to the system, H_{ad}, in order to bring the operation point into a dynamic security domain. In pseudo code, it could conceptually be described by:

Algorithm 1 Calculation of H_{ad}

Input: Operation points data

while $RoCoF > 2(Hz/s)$ **or** $FreqNadir < 47.5(Hz)$ **do**

$H_{ad.rocof}^{(i+1)} = |2 - RoCoF_i| \frac{\Delta H_{sc}}{|\Delta RoCoF_i|}$

$H_{ad.freqnadir}^{(i+1)} = |47.5 - FreqNadir_i| \frac{\Delta H_{sc}}{\Delta FreqNadir_i}$

if $H_{ad.rocof}^{(i+1)} > H_{ad.freqnadir}^{(i+1)}$ **then**

$H_{ad}^{(i+1)} = H_{ad.rocof}^{(i+1)}$

else

$H_{ad}^{(i+1)} = H_{ad.freqnadir}^{(i+1)}$

end if
end while

Where i is the iteration index and $\Delta H_{sc} = 0.1$ for the ANNs sensibility analysis.

The final amount of additional inertia to be added to the system (H_{ad}^{i+1}) match with the biggest value of additional inertia to bring both RoCoF and frequency nadir values into the security zone. Therefore, this algorithm allows changes in the control variable, for a specified operation scenario, moving the system towards its dynamic security domain, as shown in table 4.3 for one of the initial insecure operation scenarios.

Table 4.3: Initial state and new states provided by algorithm 1

i	Htotal (s)	Hsc (s)	Had (s)	RoCoF (Hz/s)	Freq. Nadir (Hz)
1	7	0	0	4.0867	46.0601
2	11.016	4.016	4.016	2.5118	46.9111
3	12.6587	5.6587	1.6427	0.9611	47.8730

As presented in the previous table, for this operating point, it was necessary two iterations to turn this initial unstable operation point in a stable one, by adding 5.6587s to the total SCs inertia constant. From the sensitivity analysis for this operation point resulted:

$$\frac{\Delta H_{sc}}{|\Delta RoCoF_i|} = \frac{0.1}{0.076066} = 1.3146 \tag{4.7}$$

$$\frac{\Delta H_{sc}}{|\Delta FreqNadir_i|} = \frac{0.1}{0.03585} = 2.7894 \tag{4.8}$$

Therefore, the initial operation point resulting from an UC and dispatch without security concerns is the algorithm input. Starting from this point, the algorithm performs a search of new stable feasible state. This search is guided, on one hand, by the derivatives 4.5 4.6 and, on the other hand, by the knowledge acquired in the system analysis phase, related with the influence of H_{sc} on RoCoF and frequency nadir values. Thus, the algorithm changes H_{sc} to decrease RoCoF and increase frequency nadir and stops when 4.3 e 4.4 are verified.

4.4 Summary

This chapter concerns the development of a real-time dynamic behavior and security evaluation tool and the derivation of preventive control actions in order to allow successful RES integration in islanded power systems. The use of such tool is important for the on-line power system operation and management, aiming to avoid load shedding after the occurrence of disturbances in the system. Regarding the ANNs performance level, it is possible to conclude that ANNs provided effective results. In fact, the reduced test errors obtained with the ANN and the illustrative cases evaluated through dynamic simulations demonstrate the quality and the feasibility of the proposed assessment tool when dealing with dynamic security problems.

Chapter 5

Results

5.1 Introduction

Previously, in chapter 3, it was presented the main methodology adopted to fulfil the purpose of this work as well as the power system's dynamic model developed in the simulation platform for dynamic studies and data set generation to be used by ANNs. In the same chapter, it was also presented a description of the power system used as case study for this work and how the feasible operation points were generated. Additionally, in chapter 4, it was presented the framework used to create two ANNs to emulate system's frequency response and to evaluate the minimum synchronous inertia required to maintain the system's stability through the algorithm developed.

Therefore, this chapter 5 aims now to present, firstly, the results of dynamic response obtained in MATLAB/SIMULINK by using the model developed for the power system for each contingency so that the results and the model could be analysed and validated in the time domain. Secondly, in section 5.3, it is presented the main results of this thesis. In this section, the ANNs emulation quality is verified and, through the use of algorithm 1 based in a sensitivity analysis, it is presented the quality of the tool developed in this work to perform a fast assessment of the dynamic behavior and to evaluate the minimum synchronous inertia to improve dynamic security in the power system.

Additionally, throughout this chapter, contingency 1 refers to wind and solar production loss and contingency 2 refers to thermal unit 1 tripping.

5.2 Dynamic Response in MATLAB/SIMULINK

The purpose of this section is to present some results regarding frequency response when the power system used as a case study experience one of the contingencies considered.

Firstly, in table 5.1, it is presented the number of insecure operation scenarios regarding each contingency, as a result of dynamic simulations performed in MATLAB/SIMULINK. From the all 102968 different operation points generated, as explained in chapter 3, 10478 of them are insecure when the power system is disturbed by contingency 1. This can be explained by the fact that

for these insecure points, wind and solar production is relatively high, satisfying between 37.5% and 61.3% of the load. Thus a loss of 50% of wind and solar production becomes a very severe disturbance to the system. Additionally, as mentioned in previous chapters, because wind and solar production plays an important role in load satisfaction, thus there are not so many conventional generators in operation to provide the necessary synchronous inertia to maintain system's security.

Regarding contingency 2, only 3106 operation scenarios revelled to be insecure. The reason for the number of insecure points be less when compared to contingency 1 is because system stability can only be put in risk when thermal unit 1 is operating, corresponding to only 10848 possible operation points.

Table 5.1: Number of insecure points for each contingency

	Contingency 1	Contingency 2
Insecure Points	10478	3106
RoCoF >2 (Hz/s)	9481	3106
Freq.Nadir <47.5 (Hz)	8392	1066
RoCoF >2 (Hz/s) and Freq.Nadir <47.5 (Hz)	7395	1066

In figures 5.1 and 5.2 it is shown the power response from thermal and hydro units when contingency 1 and 2 occur, respectively, for the following operation scenario, where wind and solar penetration is almost 54%:

Table 5.2: Operation point description

PT1	PT2	PT3	PT4	PT5	PH1
1200	0	0	0	0	1000
PH2	Wind	PV	Load	S.R.	Htotal
1400	3600	600	7800	2720	7

Where $PT1$, $PT2$, $PT3$, $PT4$ and $PT5$ are the active power output (kW) from thermal units and $PH1$ and $PH2$ are the active power output (kW) from hydro units. $S.R.$ is the spinning reserve (kW) and $Htotal$ is the total system inertia constant in seconds.
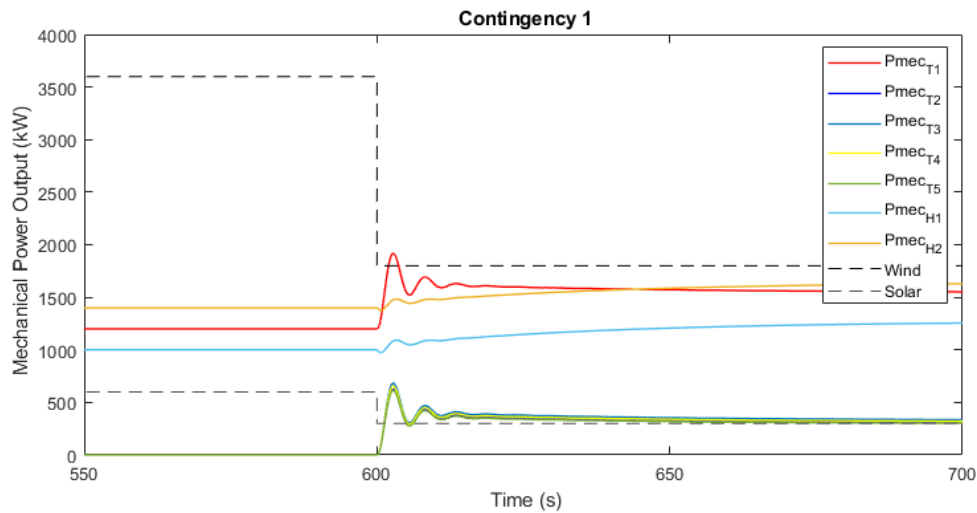
Figure 5.1: Thermal and hydro machines power response for contingency 1
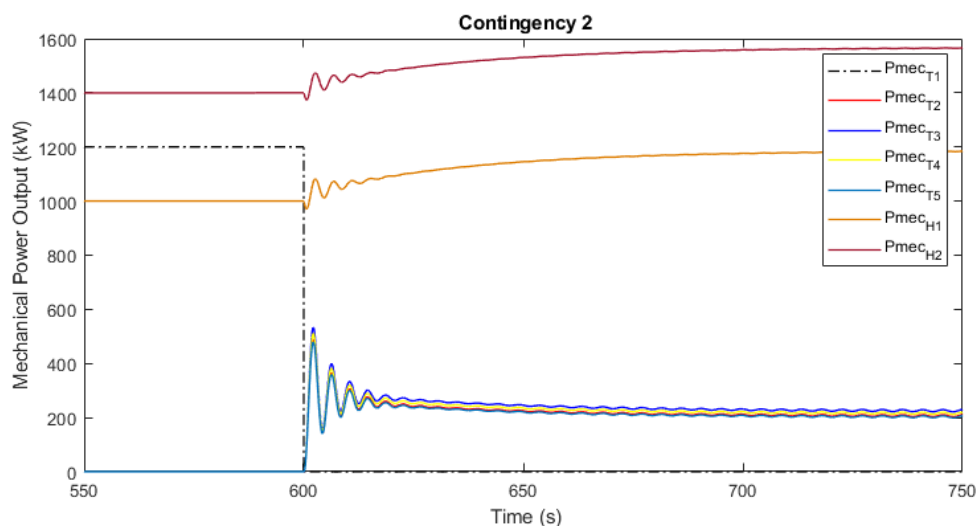
Figure 5.2: Thermal and hydro machines power response for contingency 2

In both figures it can be verified that when the disturbance occurs (at 600s) and the active power production drops, resulting from the loss of wind and solar power production (contingency 1) or from the thermal unit 1 tripping (contingency 2), the remaining synchronous machines are responsible for increasing its production, if there is an available power margin, so that the mismatch between generation and consumption could be eliminated, leading to frequency deviation elimination. Therefore, after the disturbance, the amount of additional power, resulting from the increase of power output, corresponds to the amount of power lost during the contingency. Additionally, for contingency 2, the reason for wind and solar power output not being represented in figure 5.2 is because both sources do not have frequency regulation and are modelled as a power injector, as mentioned in chapter 3, keeping its active power output constant. Moreover, it can also

be verified impact of the water starting time inertia phenomena in hydraulic turbines, as mentioned in section 3.3.2, in both situations.

The following figures, 5.3 to 5.6, presents the frequency response for both contingencies, considering the same operation scenario described in table 5.2. Firstly, it is possible to analyze the influence that SCs have on system dynamics. As mentioned in chapter 3, SCs provide additional inertia to the system, being commonly used in islanded power systems where the lack of synchronous inertia is responsible for bigger frequency deviations and instability. Therefore, in order to analyse their influence, different simulations were performed for different values of SCs inertia constant.
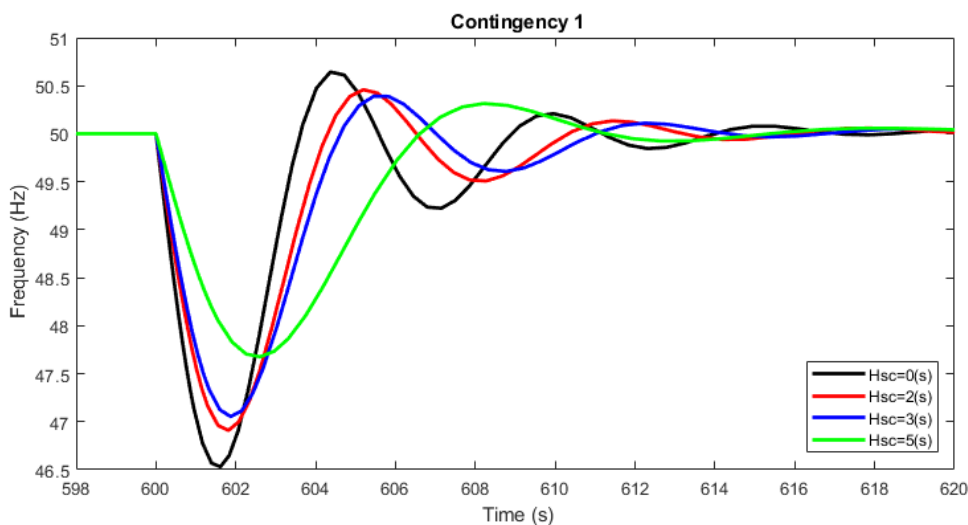
Figure 5.3: System frequency response for contingency 1
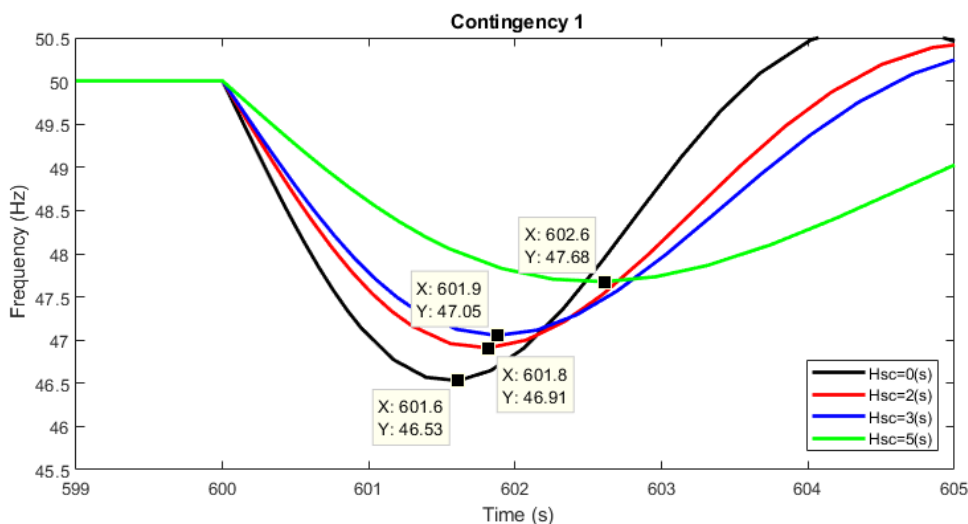
Figure 5.4: Frequency nadir for contingency 1

The results show, as expected, that the higher the inertia constant added to the system, the better the dynamic response of the system when a disturbance occurs.
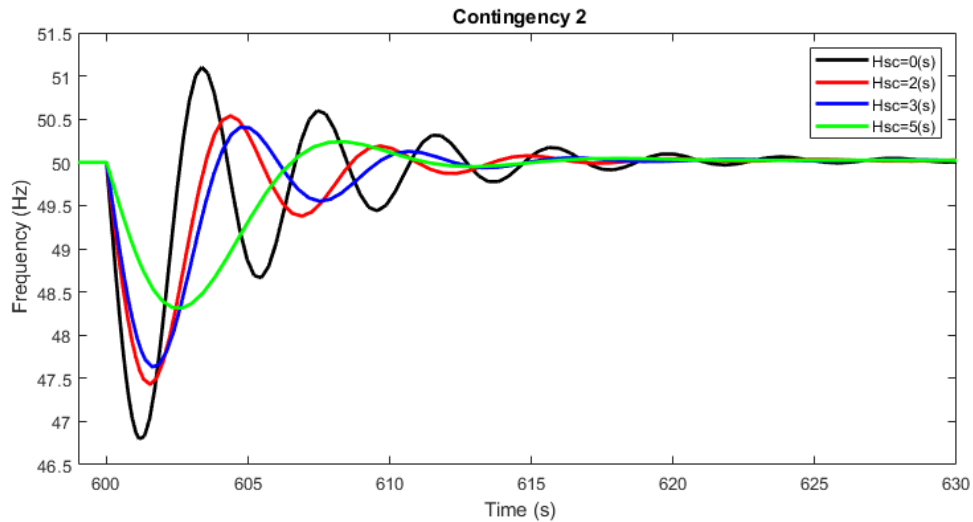
Figure 5.5: System frequency response for contingency 2
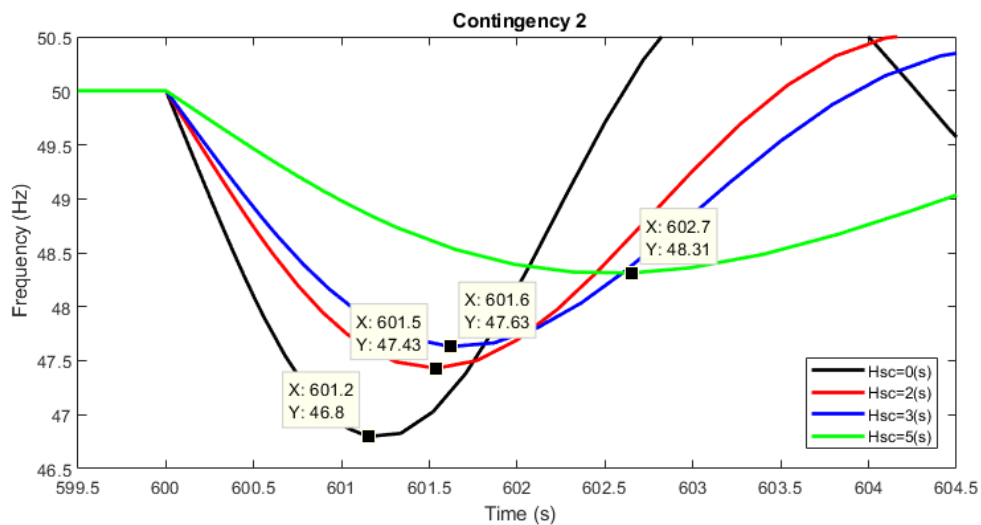
Figure 5.6: Frequency nadir for contingency 2

The results show that, for the power system used as a case study, contingency 1 is more severe than contingency 2 because the loss of wind and solar production leads to a bigger number of insecure operation points and its RoCoF and frequency deviation is bigger than in contingency 2. Due to the fact that this power system is characterized for its high wind and solar penetration, any disturbance in these sources will cause bigger frequency deviations than in systems were electric power is mainly provided by conventional power plants with frequency regulation and synchronous inertia.

Moreover, table 5.3 establishes a comparison between contingency 1 and 2 regarding maximum RoCoF value, minimum frequency nadir, as well as RoCoF and frequency nadir average values.

Table 5.3: Contingency 1 versus contingency 2

	Contingency 1	Contingency 2
Maximum RoCoF (Hz/s)	4.08706	3.95646
Minimum Freq. Nadir (Hz)	46.05416	46.79839
Average RoCoF (Hz/s)	1.23989	0.16080
Average Freq. Nadir (Hz)	48.64271	49.82978

5.3 Minimum Synchronous Inertia Evaluation

In the previous sections, the power system dynamic response for both contingencies considered in this work was presented. The purpose of this section is to present some of the results obtained during the development of this work regarding the ability of the tool developed to perform a fast dynamic security assessment and evaluate the minimum synchronous inertia to be added to the system when an insecure operation scenario is considered. Subsection 5.3.1 concerns the loss of 50% of wind and solar production and subsection 5.3.2 concerns the thermal unit 1 tripping contingency.

5.3.1 Contingency 1

In this subsection, it is presented the results obtained for one of the total operation points considered for the development of this work. This subsection aims to present the performance achieved by algorithm 1, exploited in subsection 4.3.4, in order to support the preventive control action by identifying the required minimum synchronous inertia to maintain system stable for a certain operation.

It is presented in table 5.4 the description of the operation point used for this analysis. By performing a dynamic simulation in MATLAB/SIMULINK, it is known in advance that this operation point is unstable for the RoCoF and frequency nadir margins established.

Table 5.4: Operation point description

PT1	PT2	PT3	PT4	PT5	PH1
0	0	0	0	1000	1000
PH2	Wind	PV	Load	S.R.	Htotal
900	4000	600	7500	3060	7

As a result of algorithm 1 performance, it is shown in table 5.5, the results for each iteration needed to identify the minimum synchronous inertia to move the system into the security domain.

Table 5.5: Minimum synchronous inertia for contingency 1

| i | Htotal (s) | Hsc (s) | Had (s) | ANN | | Dynamic Simulation | | RoCoF | Freq. Nadir |
				RoCoF (Hz/s)	Freq. Nadir (Hz)	RoCoF (Hz/s)	Freq. Nadir (Hz)	Abs. Diff.	Abs. Diff.
0	7	0	0	4.0867	46.0601	4.0870	46.0542	0.0003	0.0059
1	11.016	4.016	4.016	2.5118	46.9111	2.6017	47.2718	0.0899	0.3607
2	12.658	5.658	1.642	0.9611	47.8730	1.5665	47.5028	0.6054	0.3702

Considering this operation scenario, the results show that the power system needs to have a total inertia constant of 12.658 (s) in order to keep its stability when wind and solar power output drop to 2MW and 300kW, respectively. Due to the fact that in this operation scenario thermal unit 5 and hydro units 1 and 2 are in operation, the initial constant of inertia present in the system is 7(s) and therefore, there is a need of 5.658(s) of additional synchronous inertia to maintain system secure. However, it is important to mention that the inertia to be added to the system rely on SCs characteristics, and as a result, the additional inertia follows a discrete philosophy. In other words, in this case, the additional inertia should be 6(s) and not 5.658(s). Moreover, both constraints 4.3 and 4.4 are respected after algorithm 1 be performed twice.

Figure 5.7 shows the frequency response in simulation platform for each level of additional inertia. It is verified that both RoCoF and frequency deviation values are becoming lower so that the system could become dynamically secure.
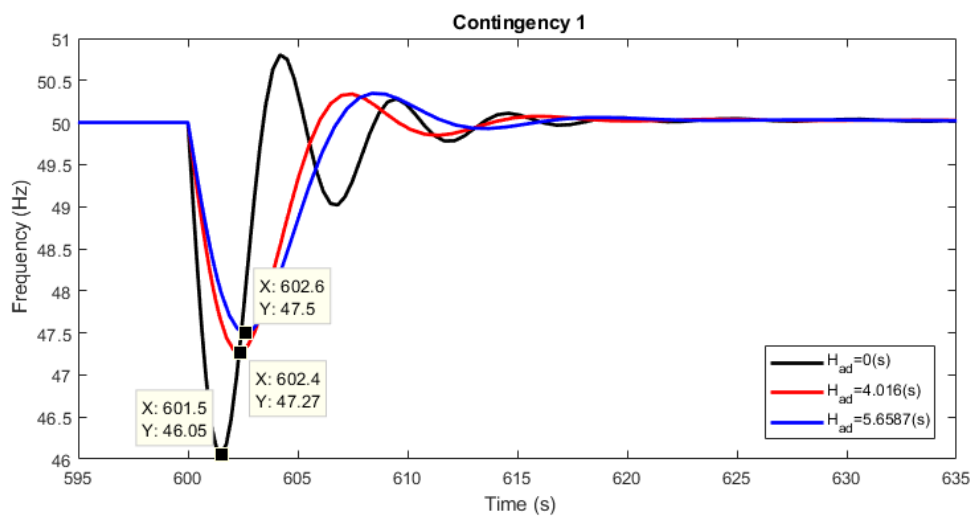

Figure 5.7: Frequency response for each level of additional inertia - contingency 1

5.3.2 Contingency 2

In this subsection it is presented the results obtained by algorithm 1, considering the contingency 2. The operation point used to evaluate the algorithm performance is described as follows:

Table 5.6: Operation point description for contingency 2

PT1	PT2	PT3	PT4	PT5	PH1
1200	0	0	0	0	1000
PH2	Wind	PV	Load	S.R.	Htotal
1400	3600	600	7800	2720	7

In table 5.7, it is presented the six iterations performed by the algorithm 1 developed in MAT-LAB/SIMULINK to performance the preventive control proposed.

Table 5.7: Minimum synchronous inertia evaluation for contingency 2

| i | Htotal (s) | Hsc (s) | Had (s) | ANN | | Dynamic Simulation | | RoCoF | Freq. Nadir |
				RoCoF (Hz/s)	Freq. Nadir (Hz)	RoCoF (Hz/s)	Freq. Nadir (Hz)	Abs. Diff.	Abs. Diff.
0	7	0	0	3.9564	46.7982	3.9565	46.7984	0.0001	0.0002
1	8.77	1.77	1.77	2.6913	47.3789	2.6972	47.3760	0.0059	0.0029
2	9.3954	2.3954	0.6254	2.4307	47.5116	2.4246	47.5141	0.0061	0.0025
3	9.7851	2.7851	0.3897	2.2858	47.5884	2.2809	47.5909	0.0049	0.0025
4	10.043	3.0437	0.2586	2.1931	47.6388	2.1946	47.6381	0.0015	0.0007
5	10.331	3.3315	0.2878	2.0902	47.6962	2.1059	47.6876	0.0157	0.0086
6	10.738	3.7382	0.4067	1.9368	47.7846	1.9922	47.7532	0.0554	0.0314

For the operation point used to analyse the performance of the algorithm to evaluate the minimum synchronous inertia needed to maintain system secure when contingency 2 occurs, the results show that it is necessary a total inertia of 10.738(s) to guarantee system stability when solar and wind sources suffer a power output drop of 50%. Therefore, there is a need of 3.7382(s) of additional synchronous inertia to achieve system stability.

Figure 5.8 shows the frequency response for each iteration. Just like happened for contingency 1, as more inertia is added to the system, the better the frequency response, where RoCoF and frequency deviation are becoming smaller.
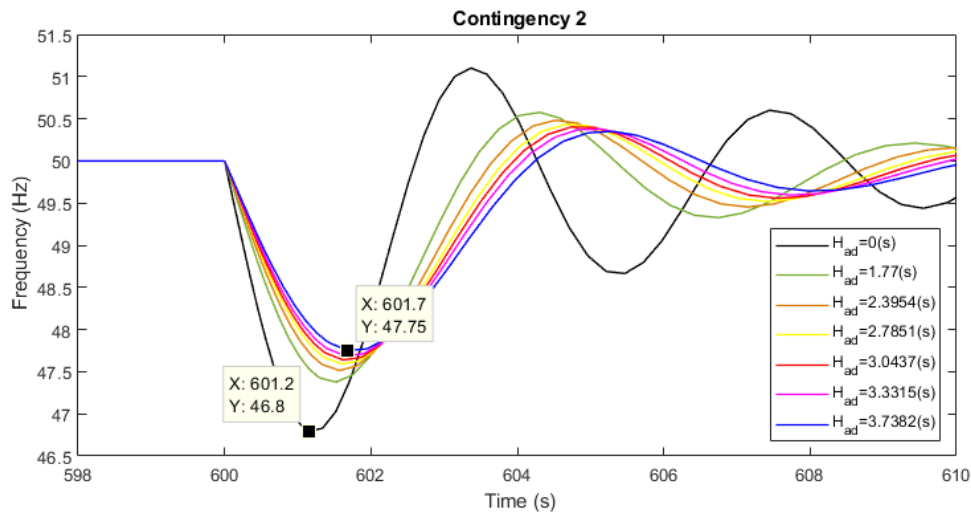
Figure 5.8: Frequency response for each level of additional inertia - contingency 2

For contingency 2, by the analysis of table 5.7 and figure 5.8, it is verified that algorithm 1 developed in MATLAB's script presents a good performance. Following the same methodology used for contingency 1, by applying the additional synchronous inertia indicated by algorithm 1 in MATLAB/SIMULINK for the same operation scenario, the system response revelled to be acceptable in terms of stability.

5.4 Summary

Some important conclusions have to be highlighted in this chapter. The first one is about the modelling of the power system used as a case study in this work. In fact, after performing several simulations for all the feasible operation points that were generated it is possible to verify that the power system was adequately modelled for frequency response analysis.

The second conclusion concerns the severity of each contingency to the system. By performing dynamic simulations for all the generated operation points in MATLAB/SIMULINK and analyzing the respective frequency response in terms of RoCoF and frequency deviation values, after subjecting the system to each disturbance, it is possible to verify that contingency 1 is the most severe contingency to the system. In fact, contingency 1 not only create more insecure operation points but also these insecure operation points have higher values of RoCoF and frequency deviations than the ones obtained for contingency 2, as shown in table 5.1.

The third conclusion is about the performance of the ANNs developed for the purpose of this work. The results shows that both ANNs have a good capacity to properly emulate system frequency response (also shown in chapter 4) and thus, be used to identify the minimum synchronous inertia required to maintain system stability when subjected to one of the disturbances studied, which is very important to accomplish the proposed goals for this thesis.

As a result, the fourth conclusion concerns the performance of the approach developed to evaluate the dynamic behavior and security of the power system for a certain operating point. The results presented in tables 5.5 and 5.7 show that algorithm 1 (using a gradient search method) was performant enough to identify, for a certain insecure operation point, the required synchronous inertia to guarantee system stability. Therefore, such tool can be used as an on-line dynamic security evaluation tool and also determine the needed preventive control actions by finding the values of the control variable (total synchronous inertia constant) that satisfy the security constraints. This will result in the mobilization of the minimum amount of SCs that bring the operating point towards a security domain.

Chapter 6

Conclusions

6.1 Conclusions

The electric power systems are envisioned to be clean, sustainable, and largely based on renewable sources interfaced with power electronics, like wind and solar resources, in the future. In contrast, the actual power systems heavily rely on conventional power plants with SGs, whose inherent physical properties are the foundation for the actual power grids stability and security. In particular, their synchronous inertia and their controls ensure dynamic stability of the power grids. As renewable generation replaces conventional generation, this foundation of the actual power systems is replaced by variable renewable sources. This results in larger and more frequent frequency deviations, jeopardizing the dynamic stability of the power systems after a disturbance.

As a result, power systems with high levels of RES penetration has more difficulties in frequency control, and the variability of wind and solar resources tend to lead to the limitation of RES integration due to the lack of synchronous inertia present in the system. Therefore, in order to avoid security issues, a very conservative policy of operation dispatch is usually adopted, leading to under exploitation of wind and solar power production.

The envisioned power systems can only be attained with the development of control systems and methodologies to perform a fast and accurate prediction of the dynamic response of the system, in real-time, providing support to the decision maker by identifying some preventive control actions so that, the limitation of RES integration and system collapse could be avoided.

The methodology developed in this work has the purpose of evaluate the dynamic security of an islanded power system with high RES integration, considering a certain operation scenario when power system is subject to the loss of half of the wind and solar production or when the biggest thermal unit tripping occurs, and identify the minimum synchronous inertia required to maintain system security when one of these disturbances occurs.

After several simulations for different operation scenarios and disturbances, the developed tool proved to be able to identify the minimum synchronous inertia that must be present in the system to avoid load shedding or even system collapse when an operation scenario, heavily based on wind and solar generation is exploited. As a result, through its ability for fast and accurately evaluate

the minimum required inertia, this tool provides to the system operator the value of additional inertia constant that must be added to the system in order to ensure the dynamic security of the system. By that, the system operator can adopt preventive actions such as the activation of SCs to deliver the required additional synchronous inertia to the system. The use of ANNs proved to be essential for the success of this tool since they provide a faster security evaluation than simulation platforms without compromising the evaluation accuracy.

The main contribution of this work lies in the possibility of real-time preventive measures in terms of SCs activation, in case of instability detection, can be suggested by exploiting the possibility of getting, directly from a trained ANN, the sensitivities of the stability indexes relative to system variables, as ANN inputs.

6.2   Future Work

The work developed in this thesis provides insight on operational and control systems based on fast dynamic response prediction capacity, useful to manage power systems with high levels of renewable energy penetration.

Beyond the contributions brought by this thesis, additional simulations are required in order to improve the performance and the flexibility of the methodology developed. As a suggestion, some of those simulations not tackled in this thesis but envisioned by its relevance, for successful integration of RES in power grids are:

- Perform dynamic studies in power systems with lower inertia constant so that RoCoF values could be higher than the ones achieved in this work. This way, dynamic security could be evaluated for systems where wind and solar integration would be even higher (a future trend in the electric power sector);

- Other disturbances could be simulated to study the frequency response of the system so that a more robust and flexible assessment tool could be achieved and, therefore, a wide range of possible scenarios and conditions could be covered;

Additionally, the work developed has some limitations that must be addressed. The model of the power system created in MATLAB/SIMULINK does not consider the wind generator model. Moreover, because the developed model is based on a single bus philosophy, this model is very simplistic when compared with real islanded power systems. Nevertheless, the results have proved to be very acceptable.

For future work, it is also recommendable that for studying the thermal unit tripping contingency, more operation scenarios with the correspondent thermal unit in operation would be generated so that, more knowledge for ANN training could be achieved leading to better performance from this ANN.

Appendix A

Power System's MATLAB/SIMULINK Model and Parameters

All the tables and figures presented in this appendix contain all the necessary parameters and data, as well as the complete and detailed model developed and performed in MATLAB/SIMULINK so that the results could be reproduced, checked and be helpful for possible future work.

Therefore, in sections A.1 and A.2, it is presented the parameters of thermal and hydro units, respectively. In sections A.3 and A.4, it is presented the complete power system's model for dynamic studies in MATLAB/SIMULINK platform for contingency 1 and 2, respectively.

A.1 Thermal Units Parameters

Table A.1: Parameters of the thermal units

Thermal Units	
Parameter	Value
R	0.25 p.u.
Integral Gain	1
Tg	0.1 s
Ta	1 s

A.2   Hydro Units Parameters

Table A.2: Parameters of the hydro units

Hydro Units	
Parameter	Value
R	0.25 p.u.
Integral Gain	1
Tg	0.1 s
Tw	1 s
Tr	5 s
r	10 p.u.

A.3   Dynamic Model in MATLAB/SIMULINK

In figure A.1, it is presented the model developed in the simulation platform for the power system used as a case study. Both thermal (grey) and hydro units (blue) are represented through MATLAB/SIMULINK's subsystems (masks) to simplify the model layout. Inside these masks, frequency regulation loops are modelled as presented in figures 3.6 and 3.7 in chapter 3. This model is used in order to study system dynamic behavior for contingency 1. Therefore, wind (white) and solar (yellow) blocks have a power output modelled as shown in figures 3.16 and 3.17 in chapter 3.

Additionally, this single bus model has an equivalent swing equation (light green) with two parameters: system equivalent inertia constant, H_{eq}, and the equivalent damping constant, D_{eq}. H_{eq} value is dependent of the number of thermal and/or hydro units that are in operation for a certain operation scenario, as well as the load value and the power of each generation unit and wind and solar power plants. D_{eq} is assumed to be always 2 p.u.
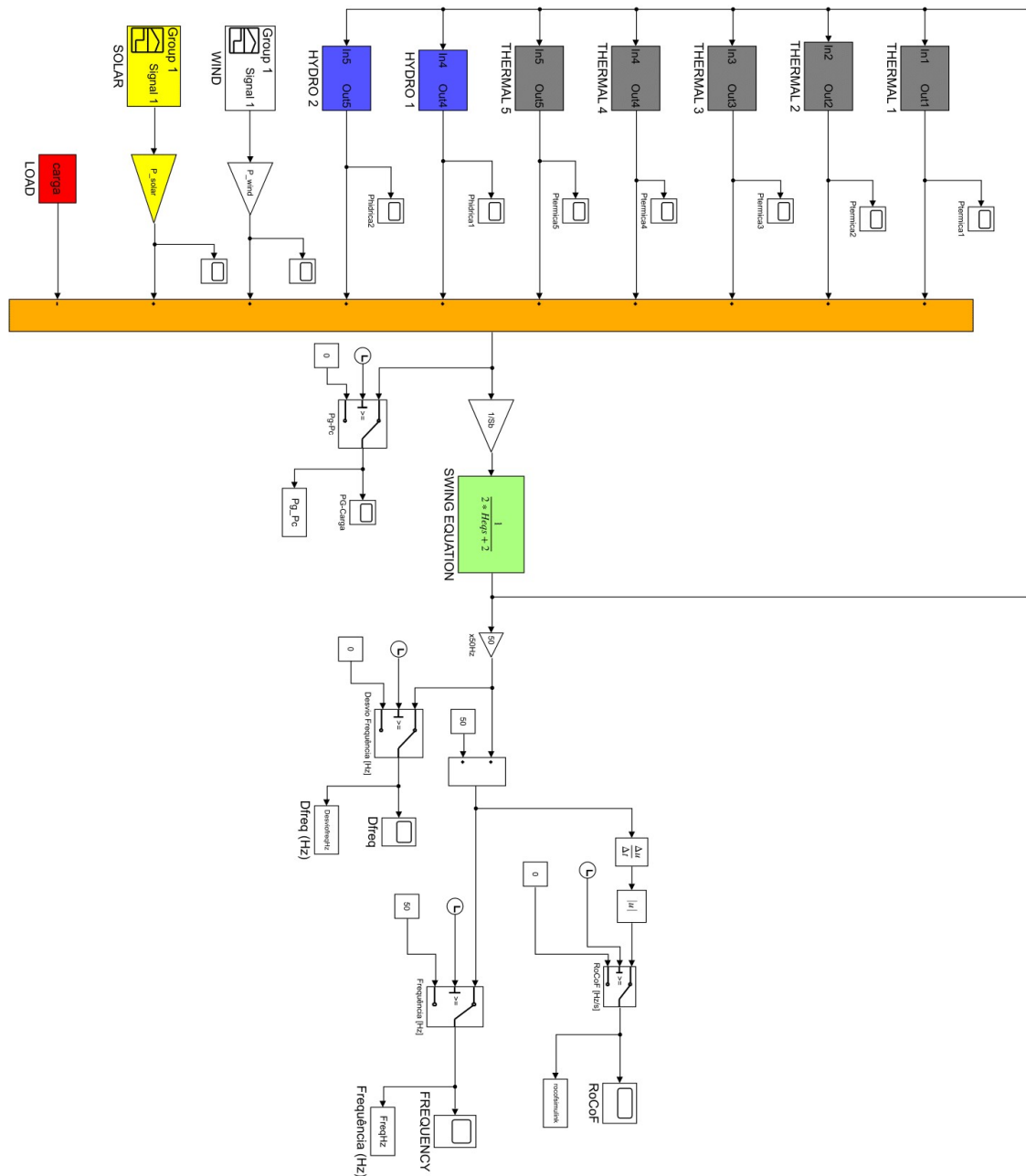
Figure A.1: Power System's Dynamic Model

A.4   Dynamic Model for Contingency 2

The following model, figure A.2, is used to perform dynamic studies for contingency 2. This model is similar to the original model used for contingency 1, however, due to the fact that this contingency concerns the thermal unit tripping, it is necessary to apply some changes to the model. When thermal unit 1 tripping occurs at 600 seconds of simulation, its power output must change to zero and thus, a switch (pink) is applied to change the power output in accordance. As a result

of this contingency, H_{eq} becomes smaller, and therefore, the same strategy is applied to the swing equation block. When thermal unit 1 tripping occurs, system inertia constant changes from H_{eq} to H_{eqd}, at 600 seconds. Moreover, contrarily to what happens in the first model, in this model, wind and solar power output is constant and equal to the power dispatch result.

Figure A.2: Power System's Dynamic Model for contingency 2

References

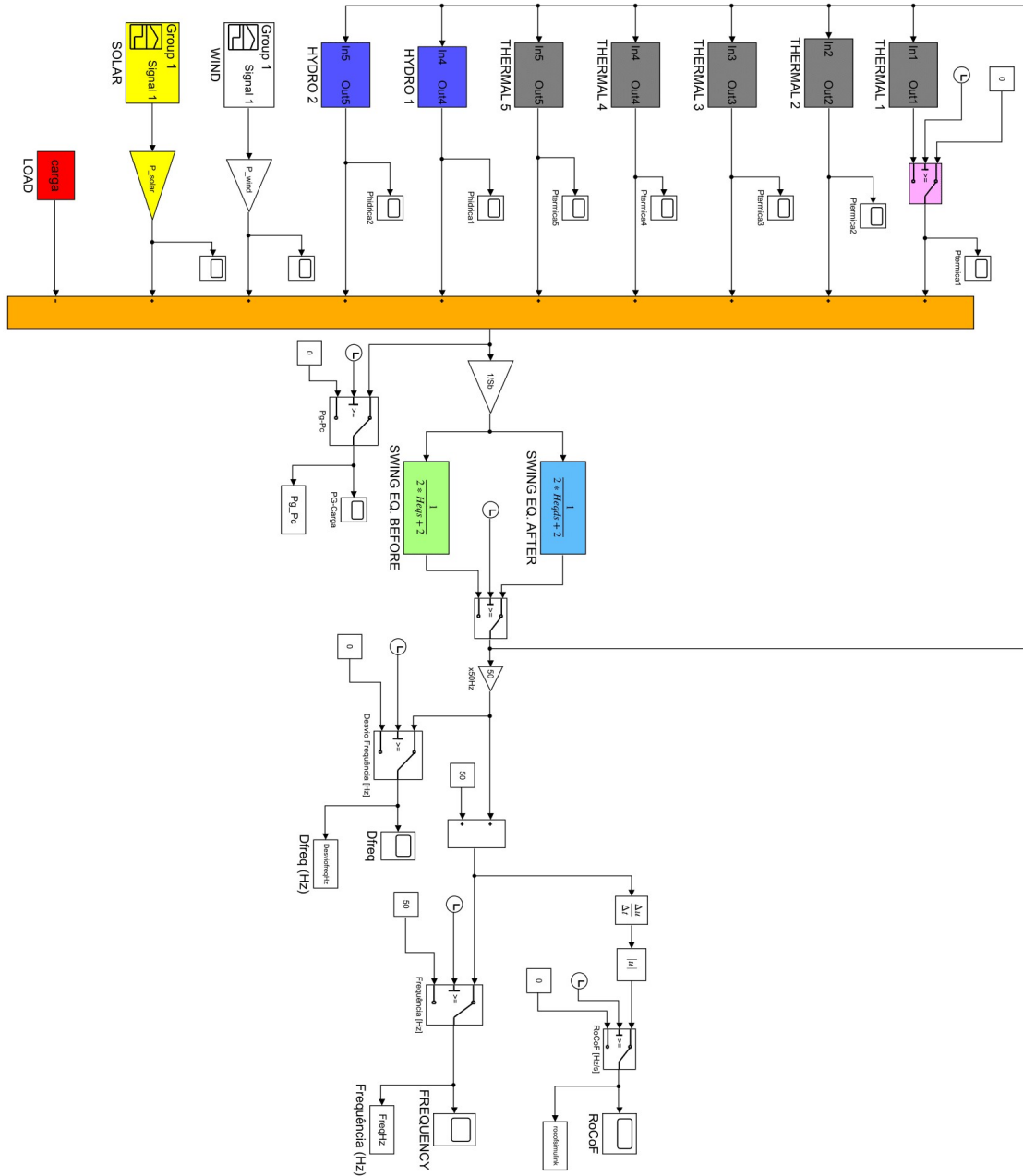[1] Jan Van De Vyver, Jeroen D.M. De Kooning, Bart Meersman, Lieven Vandevelde, and Tine L. Vandoorn. Droop Control as an Alternative Inertial Response Strategy for the Synthetic Inertia on Wind Turbines. *IEEE Transactions on Power Systems*, 31(2):1129–1138, 2016. `doi:10.1109/TPWRS.2015.2417758`.

[2] Federico Milano, Florian Dorfler, Gabriela Hug, David J. Hill, and Gregor Verbič. Foundations and challenges of low-inertia systems (Invited Paper). *20th Power Systems Computation Conference, PSCC 2018*, pages 1–25, 2018. `doi:10.23919/PSCC.2018.8450880`.

[3] Francisco M. Gonzalez-Longatt. Effects of the synthetic inertia from wind power on the total system inertia: Simulation study. *2nd International Symposium on Environment Friendly Energies and Applications, EFEA 2012*, pages 389–395, 2012. `doi:10.1109/EFEA.2012.6294049`.

[4] Mircea Dulau and Dorin Bica. Simulation of Speed Steam Turbine Control System. *Procedia Technology*, 12:716–722, 2014. URL: `http://dx.doi.org/10.1016/j.protcy.2013.12.554`, `doi:10.1016/j.protcy.2013.12.554`.

[5] Ujjwol Tamrakar, Dipesh Shrestha, Manisha Maharjan, Bishnu Bhattarai, Timothy Hansen, and Reinaldo Tonkoski. Virtual Inertia: Current Trends and Future Directions. *Applied Sciences*, 7(7):654, 2017. URL: `http://www.mdpi.com/2076-3417/7/7/654`, `doi:10.3390/app7070654`.

[6] Yuan Zhang Sun, Zhao Sui Zhang, Guo Jie Li, and Jin Lin. Review on frequency control of power systems with wind power penetration. *2010 International Conference on Power System Technology: Technological Innovations Making Power Grid Smarter, POWERCON2010*, pages 1–8, 2010. `doi:10.1109/POWERCON.2010.5666151`.

[7] Mohammad Dreidy, H. Mokhlis, and Saad Mekhilef. Inertia response and frequency control techniques for renewable energy sources: A review. *Renewable and Sustainable Energy Reviews*, 69(November 2015):144–155, 2017. URL: `http://dx.doi.org/10.1016/j.rser.2016.11.170`, `doi:10.1016/j.rser.2016.11.170`.

[8] R G de Almeida and J A P Lopes. Primary frequency control participation provided by doubly fed induction wind generators. *15th PSCC, Liege*, (August):22–26, 2005. `arXiv:1206.4363`, `doi:10.1063/1.4760274`.

[9] RG De Almeida and JA Peas Lopes. Participation of doubly fed induction wind generators in system frequency regulation. *IEEE Transactions on Power Systems*, 22(3):944–950, 2007. URL: `http://ieeexplore.ieee.org/xpls/abs{_}all.jsp?arnumber=4282019`, `doi:10.1109/TPWRS.2007.901096`.

[10] P.P. Zarina, S. Mishra, and P.C. Sekhar. *Photovoltaic system based transient mitigation and frequency regulation.* IEEE, 2012. URL: https://www.engineeringvillage.com/search/doc/abstract.url?{&}pageType=quickSearch{&}usageZone=resultslist{&}usageOrigin=searchresults{&}searchtype=Quick{&}SEARCHID=9d3d7f5a9c6e4d74b64a17878ea10d71{&}DOCINDEX=1{&}ignore{_}docid=inspec{_}ef550213da78d1e8cM54cb2061377553{&}dat.

[11] P. P. Zarina, S. Mishra, and P. C. Sekhar. Exploring frequency control capability of a PV system in a hybrid PV-rotating machine-without storage system. *International Journal of Electrical Power and Energy Systems*, 60:258–267, 2014. URL: http://dx.doi.org/10.1016/j.ijepes.2014.02.033, doi:10.1016/j.ijepes.2014.02.033.

[12] M. Nedd, C. Booth, and K. Bell. Potential solutions to the challenges of low inertia power systems with a case study concerning synchronous condensers. *2017 52nd International Universities Power Engineering Conference, UPEC 2017*, 2017-Janua:1–6, 2017. doi:10.1109/UPEC.2017.8232001.

[13] Rui Zhang, Yan Xu, Zhao Yang Dong, Ke Meng, and Zhao Xu. Intelligent Systems for Power System Dynamic Security Assessment : Review and Classification. *2011 4th International Conference on Electric Utility Deregulation and Restructuring and Power Technologies (DRPT)*, pages 134–139, 2011. doi:10.1109/DRPT.2011.5993876.

[14] P. Morison, K.; Lei Wang; Kundur. Power system security assessment. 2:30–39, 2004.

[15] Prabha Kundur. Power System Stability And Control, 1993.

[16] European Comission. Analysis of options beyond 20% GHG emission reductions: Member State results. pages 1–49, 2012.

[17] European Council. Conclusions adopted by the European Council meeting. EUCO 169/14 ON THE 2030 Climate and Energy Policy Framework. (October), 2014. URL: http://data.consilium.europa.eu/doc/document/ST-169-2014-INIT/en/pdf.

[18] P. Kundur and J. Paserba and V. Ajjarapu and G. Andersson and A. Bose and C. Canizares and N. Hatziargyriou and D. Hill and A. Stankovic and C. Taylor and T. Van Cutsem and V. Vittal. Definition and classification of power system stability. *IEEE Transactions on Power Systems*, 19(June):1387–1401, 2004. doi:10.1109/TPWRS.2004.825981.

[19] Pieter Tielens and Dirk Van Hertem. The relevance of inertia in power systems. *Renewable and Sustainable Energy Reviews*, 55(2016):999–1009, 2016. URL: http://dx.doi.org/10.1016/j.rser.2015.11.016, doi:10.1016/j.rser.2015.11.016.

[20] R.A. Serway. *Physics for Scientists and Engineers*. 1989.

[21] Peter Wall, Francisco Gonzalez-Longatt, and Vladimir Terzija. Estimation of generator inertia available during a disturbance. *IEEE Power and Energy Society General Meeting*, pages 1–8, 2012. doi:10.1109/PESGM.2012.6344755.

[22] Ronan Doherty, Student Member, Gillian Lalor, Student Member, Mark O Malley, and Senior Member. Frequency Control in Competitive Electricity Market Dispatch. 20(3):1588–1596, 2005.

[23] Sandip Sharma, Shun Hsien Huang, and N. D.R. Sarma. System inertial frequency response estimation and impact of renewable resources in ERCOT interconnection. *IEEE Power and Energy Society General Meeting*, pages 1–6, 2011. `doi:10.1109/PES.2011.6038993`.

[24] Ahmad Shabir Ahmadyar, Shariq Riaz, Gregor Verbic, Archie Chapman, and David J. Hill. A Framework for Assessing Renewable Integration Limits with Respect to Frequency Performance. *IEEE Transactions on Power Systems*, 33(4):4444–4453, 2018. `doi:10.1109/TPWRS.2017.2773091`.

[25] Berardino Porretta and Steven Porretta. Calculation of power systems inertia and frequency response. *2018 IEEE Texas Power and Energy Conference, TPEC 2018*, 2018-Febru:1–6, 2018. `doi:10.1109/TPEC.2018.8312111`.

[26] Yann G. Rebours, Daniel S. Kirschen, Marc Trotignon, and Sebastien Rossignol. A Survey of Frequency and Voltage Control Ancillary Services - Part I: Technical Features. *IEEE Transactions on Power Systems*, 22(1):350–357, 2007. `doi:10.1109/TPWRS.2006.888963`.

[27] P. W. Sauer and M. A. Pai. *Power System Dynamics and Stability*. 1998.

[28] L.H. Fink, N. Jaleeli, L.S. VanSlyck, D.N. Ewart, and A.G. Hoffmann. Understanding automatic generation control. *IEEE Transactions on Power Systems*, 7(3):1106–1122, 2002. `doi:10.1109/59.207324`.

[29] J.B. Ekanayake, N. Jenkins, and G. Strbac. Frequency Response from Wind Turbines. *Wind Engineering*, 32(6):573–586, 2009. `doi:10.1260/030952408787548811`.

[30] Corbetta Giorgio, Andrew Ho, and Ivan Pineda. Wind energy scenarios for 2030. *Ewea*, (July):1–8, 2015. URL: `http://www.ewea.org/fileadmin/files/library/publications/reports/EWEA-Wind-energy-scenarios-2030.pdf`, `arXiv:arXiv:1011.1669v3`, `doi:10.1017/CBO9781107415324.004`.

[31] Solar Power Europe. Global Market Outlook for Solar Power. Technical report, 2018. URL: `http://www.solarpowereurope.org`.

[32] Huajie Gu, Ruifeng Yan, and Tapan Kumar Saha. Minimum Synchronous Inertia Requirement of Renewable Power Systems. *IEEE Transactions on Power Systems*, 33(2):1533–1543, 2018. `doi:10.1109/TPWRS.2017.2720621`.

[33] Huajie Gu. Maximum instantaneous renewable energy integration of power grids. In *2016 Australasian Universities Power Engineering Conference (AUPEC)*, pages 1–5. IEEE, 2016. URL: `http://ieeexplore.ieee.org/document/7749368/`, `doi:10.1109/AUPEC.2016.7749368`.

[34] Pengfei Li, Weihao Hu, and Zhe Chen. Review on integrated-control method of variable speed wind turbines participation in primary and secondary frequency. *IECON Proceedings (Industrial Electronics Conference)*, pages 4223–4228, 2016. `doi:10.1109/IECON.2016.7794127`.

[35] Til Kristian Vrana, J. Charles Smith, Nicolaos Cutululis, Damian Flynn, Juha Kiviluoma, Davy Marcel, and Emilio Gomez-Lazaro. Wind power within European grid codes: Evolution, status and outlook. *Wiley Interdisciplinary Reviews: Energy and Environment*, 7(3):e285, 2018. `doi:10.1002/wene.285`.

[36] Bogdan Ionuţ Crăciun, Tamás Kerekes, Dezso Séra, and Remus Teodorescu. Overview of recent drid codes for PV power integration. *Proceedings of the International Conference on Optimisation of Electrical and Electronic Equipment, OPTIM*, pages 959–965, 2012. doi:10.1109/OPTIM.2012.6231767.

[37] Qianwei Zheng, Jiaming Li, Xiaomeng Ai, Jinyu Wen, and Jiakun Fang. Overiew of grid codes for photovoltaic integration. *2017 IEEE Conference on Energy Internet and Energy System Integration, EI2 2017 - Proceedings*, 2018-Janua:1–6, 2018. doi:10.1109/EI2.2017.8245501.

[38] Arani M.F.M. and El-Saadany E.F. Implementing virtual inertia in DFIG-based wind power generation. *IEEE Transactions on Power Systems*, 28(2):1373–1384, 2013. URL: http://www.scopus.com/inward/record.url?eid=2-s2.0-84886446794{&}partnerID=40{&}md5=f43240d239236849de7416b228c1c4b3, doi:10.1109/TPWRS.2012.2207972.

[39] Danny Ochoa and Sergio Martinez. Fast-Frequency Response Provided by DFIG-Wind Turbines and its Impact on the Grid. *IEEE Transactions on Power Systems*, 32(5):4002–4011, 2017. doi:10.1109/TPWRS.2016.2636374.

[40] Juan Manuel Mauricio, Student Member, Alejandro Marano, Antonio Gómez-expósito, José Luis, Martínez Ramos, and Senior Member. Variable-Speed Wind Energy Conversion Systems. *Power*, 24(1):173–180, 2009. doi:10.1109/TPWRS.2008.2009398.

[41] Jiebei Zhu, Djaved Rostom, Chavdar Ivanov, Amir Dahresobh, Richard Ierna, and Helge Urdal. System strength considerations in a converter dominated power system. *IET Renewable Power Generation*, 9(1):10–17, 2014. doi:10.1049/iet-rpg.2014.0199.

[42] Tianqi Hong and Francisco De León. Controlling non-synchronous microgrids for load balancing of radial distribution systems. *IEEE Transactions on Smart Grid*, 8(6):2608–2616, 2017. doi:10.1109/TSG.2016.2531983.

[43] Shuo Wang, Jiabing Hu, Xiaoming Yuan, and Li Sun. On Inertial Dynamics of Virtual-Synchronous-Controlled DFIG-Based Wind Turbines. *IEEE Transactions on Energy Conversion*, 30(4):1691–1702, 2015. doi:10.1109/TEC.2015.2460262.

[44] Shuo Wang, Jiabing Hu, Shuai Li, and Wenming Tang. Full-capacity wind turbine with inertial support by optimizing phase-locked loop. (Vc):5 .–5 ., 2016. doi:10.1049/cp.2015.0431.

[45] Ömer Göksu, Remus Teodorescu, Claus Leth Bak, Florin Iov, and Philip Carne Kjær. Instability of wind turbine converters during current injection to low voltage grid faults and PLL frequency based stability solution. *IEEE Transactions on Power Systems*, 29(4):1683–1691, 2014. doi:10.1109/TPWRS.2013.2295261.

[46] Federico Bizzarri, Angelo Brambilla, and Federico Milano. Analytic and numerical study of TCSC devices: Unveiling the crucial role of phase-locked loops. *IEEE Transactions on Circuits and Systems I: Regular Papers*, 65(6):1840–1849, 2018. doi:10.1109/TCSI.2017.2768220.

[47] Jingyang Fang, Ruiqi Zhang, Yi Tang, and Li Hongchang. Inertia Enhancement by Grid-Connected Power Converters with Frequency-Locked-Loops for Frequency Derivative Estimation. *IEEE Power and Energy Society General Meeting*, 2018-Augus:1–5, 2018. doi:10.1109/PESGM.2018.8586213.

[48] Sebastian Curi, Dominic Groß, and D Florian. Control of Low Inertia Power Grids: A Model Reduction Approach. (Cdc):5708–5713, 2017.

[49] Charles K. Sao and Peter W. Lehn. Control and power management of converter fed microgrids. *IEEE Transactions on Power Systems*, 23(3):1088–1098, 2008. `doi:10.1109/TPWRS.2008.922232`.

[50] Ali Mehrizi-Sani and Reza Iravani. Potential-function based control of a microgrid in islanded and grid-connected modes. *IEEE Transactions on Power Systems*, 25(4):1883–1891, 2010. `doi:10.1109/TPWRS.2010.2045773`.

[51] Ieee Transactions, O N Power, and F Katiraei. Power Management Strategies for a Microgrid With. 21(April 2016):1821–1831, 2006. `doi:10.1109/TPWRS.2006.879260`.

[52] Ahmadreza Tabesh and Reza Iravani. Multivariable Dynamic Model and Robust Control of a Voltage-Source Converter for Power System Applications. *IEEE Transactions on Power Delivery*, 24(1):462–471, 2009. URL: `http://ieeexplore.ieee.org/document/4512043/`, `doi:10.1109/TPWRD.2008.923531`.

[53] G. Denis, T. Prevost, P. Panciatici, X. Kestelyn, F. Colas, and X. Guillaud. Review on potential strategies for transmission grid operations based on power electronics interfaced voltage sources. *IEEE Power and Energy Society General Meeting*, 2015-Septe:1–5, 2015. `doi:10.1109/PESGM.2015.7286111`.

[54] Uros Markovic, Petros Aristidou, and Gabriela Hug. Virtual Induction Machine Strategy for Converters in Power Systems with Low Rotational Inertia. *10th Bulk Power Systems Dynamics and Control Symposium*, page (In Press), 2017.

[55] Junru Chen, Muyang Liu, Cathal Oloughlin, Federico Milano, and Terence Odonnell. Modelling, simulation and hardware-in-the-loop validation of virtual synchronous generator control in low inertia power system. *20th Power Systems Computation Conference, PSCC 2018*, 3, 2018. `doi:10.23919/PSCC.2018.8442998`.

[56] Qing-Chang Zhong, Phi-Long Nguyen, Zhenyu Ma, and Wanxing Sheng. Self-Synchronized Synchronverters: Inverters Without a Dedicated Synchronization Unit. *IEEE Transactions on Power Electronics*, 29(2):617–630, 2013. `doi:10.1109/tpel.2013.2258684`.

[57] Dominic Groß, Saverio Bolognani, Bala Kameshwar Poolla, and Florian Dörfler. Increasing the Resilience of Low-inertia Power Systems by Virtual Inertia and Damping. *IREP Bulk Power Systems Dynamics and Control Symposium*, pages 1–12, 2017.

[58] Andre Luna, Ujjwol Tamrakar, Timothy M. Hansen, and Reinaldo Tonkoski. Frequency Response in Grids with High Penetration of Renewable Energy Sources. *2018 North American Power Symposium, NAPS 2018*, pages 1–5, 2019. `doi:10.1109/NAPS.2018.8600620`.

[59] Pieter Tielens, Simon De Rijcke, Kailash Srivastava, Muhamad Reza, Antonis Marinopoulos, and Johan Driesen. Frequency support by wind power plants in isolated grids with varying generation mix. *IEEE Power and Energy Society General Meeting*, pages 1–8, 2012. `doi:10.1109/PESGM.2012.6344690`.

[60] M. P.N. Van Wesenbeeck, S. W.H. De Haan, P. Varela, and K. Visscher. Grid tied converter with virtual kinetic storage. *2009 IEEE Bucharest PowerTech: Innovative Ideas Toward the Electrical Grid of the Future*, (1):1–7, 2009. `doi:10.1109/PTC.2009.5282048`.

[61] Jaber Alipoor, Yushi Miura, and Toshifumi Ise. Power system stabilization using virtual synchronous generator with alternating moment of inertia. *IEEE Journal of Emerging and Selected Topics in Power Electronics*, 3(2):451–458, 2015. `doi:10.1109/JESTPE.2014.2362530`.

[62] Qing Chang Zhong and George Weiss. Synchronverters: Inverters that mimic synchronous generators. *IEEE Transactions on Industrial Electronics*, 58(4):1259–1267, 2011. `doi:10.1109/TIE.2010.2048839`.

[63] Sjoerd W. H. de Haan, Johan Morren, J. A. Ferreira, and Wil L. Kling. Wind Turbines Emulating Inertia and Supporting Primary Frequency Control. *IEEE Transactions on Power Systems*, 21(1):433–434, 2006. URL: `http://ieeexplore.ieee.org/lpdocs/epic03/wrapper.htm?arnumber=1583744`, `doi:10.1109/TPWRS.2005.861956`.

[64] Gustavo Revel, Andres E. Leon, Diego M. Alonso, and Jorge L. Moiola. Dynamics and stability analysis of a power system with a PMSG-based wind farm performing ancillary services. *IEEE Transactions on Circuits and Systems I: Regular Papers*, 61(7):2182–2193, 2014. `doi:10.1109/TCSI.2014.2298281`.

[65] J Ekanayake and N Jenkins. Comparison of the response of doubly fed and fixed-speed induction generator wind turbines to changes in network frequency. *IEEE Transactions on Energy Conversion*, 19(4):800–802, 2004. `doi:10.1109/TEC.2004.827712`.

[66] Alfred Wachtel, Stephan, and Beekmann. Contribution of wind energy converters with inertia emulation to frequency control and frequency stability in power systems. 2009.

[67] A. Teninge, C. Jecu, D. Roye, S. Bacha, J. Duval, and R. Belhomme. Contribution to frequency control through wind turbine inertial energy storage. *IET Renewable Power Generation*, 3(3):358, 2009. `doi:10.1049/iet-rpg.2008.0078`.

[68] J. Duval and B. Meyer. Frequency behavior of grid with high penetration rate of wind generation. *2009 IEEE Bucharest PowerTech: Innovative Ideas Toward the Electrical Grid of the Future*, pages 1–6, 2009. `doi:10.1109/PTC.2009.5282198`.

[69] N. Janssens, N.A. ; Lambin, G. ; Bragard. *2007 IEEE Lausanne Power Tech : proceedings, 1-5 July 2007, Lausanne, Switzerland*. IEEE, 2007. URL: `https://www.engineeringvillage.com/search/doc/abstract.url?{&}pageType=quickSearch{&}usageZone=resultslist{&}usageOrigin=searchresults{&}searchtype=Quick{&}SEARCHID=52eee08206764766986a42730854cd9f{&}DOCINDEX=1{&}ignore{_}docid=inspec{_}129f3b511b46186dcdM64682061377553{&}da`.

[70] Emmanouil Loukarakis, Ioannis Margaris, and Panayiotis Moutis. Frequency control support and participation methods provided by wind generation. In *2009 IEEE Electrical Power & Energy Conference (EPEC)*, pages 1–6. IEEE, oct 2009. URL: `http://ieeexplore.ieee.org/document/5420771/`, `doi:10.1109/EPEC.2009.5420771`.

[71] Panayiotis Moutis, Emmanouil Loukarakis, Stavros Papathanasiou, and Nikos D. Hatziargyriou. Primary load-frequency control from pitch-controlled wind turbines. In *2009 IEEE Bucharest PowerTech*, pages 1–7. IEEE, jun 2009. URL: `http://ieeexplore.ieee.org/document/5281819/`, `doi:10.1109/PTC.2009.5281819`.

[72] N. Ekanayake J. Jenkins. Control of DFIG wind turbines. *Power Engineer*, 17(February):28–32, 2003. `doi:10.1049/pe:20030107`.

[73] L. Holdsworth, J. B. Ekanayake, and N. Jenkins. Power system frequency response from fixed speed and doubly fed induction generator-based wind turbines. *Wind Energy*, 7(1):21–35, 2004. `doi:10.1002/we.105`.

[74] Xue Yingcheng and Tai Nengling. Review of contribution to frequency control through variable speed wind turbine. *Renewable Energy*, 36(6):1671–1677, 2011. URL: `http://dx.doi.org/10.1016/j.renene.2010.11.009`, `doi:10.1016/j.renene.2010.11.009`.

[75] James F. Conroy and Rick Watson. Frequency response capability of full converter wind turbine generators in comparison to conventional generation. *IEEE Transactions on Power Systems*, 23(2):649–656, 2008. `doi:10.1109/TPWRS.2008.920197`.

[76] Lu Miao, Jinyu Wen, Hailian Xie, Chengyan Yue, and Wei-Jen Lee. Coordinated control strategy of wind turbine generator and energy storage equipment for frequency support BT - 2014 IEEE Industry Application Society Annual Meeting, IAS 2014, October 5, 2014 - October 9, 2014. *2014 IEEE Industry Application Society Annual Meeting*, 51(4):2732–2742, 2014. URL: `http://dx.doi.org/10.1109/IAS.2014.6978370`, `doi:10.1109/IAS.2014.6978370`.

[77] Francisco Díaz-González, Melanie Hau, Andreas Sumper, and Oriol Gomis-Bellmunt. Coordinated operation of wind turbines and flywheel storage for primary frequency control support. *International Journal of Electrical Power and Energy Systems*, 68:313–326, 2015. `doi:10.1016/j.ijepes.2014.12.062`.

[78] P. P. Zarina, Sukumar Mishra, and P. C. Sekhar. Deriving inertial response from a non-inertial PV system for frequency regulation. *PEDES 2012 - IEEE International Conference on Power Electronics, Drives and Energy Systems*, pages 1–5, 2012. `doi:10.1109/PEDES.2012.6484409`.

[79] Rijo Rajan and Francis M. Fernandez. Fuzzy Based Control of Grid-Connected Photovoltaic System for Enhancing System Inertial Response. *Proceedings - 2018 53rd International Universities Power Engineering Conference, UPEC 2018*, pages 1–6, 2018. `doi:10.1109/UPEC.2018.8542008`.

[80] Huanhai Xin, Yun Liu, Zhen Wang, Deqiang Gan, and Taicheng Yang. A new frequency regulation strategy for photovoltaic systems without energy storage. *IEEE Transactions on Sustainable Energy*, 4(4):985–993, 2013. `doi:10.1109/TSTE.2013.2261567`.

[81] Venkata Ajay Kumar Pappu, Badrul Chowdhury, and Ravi Bhatt. Implementing frequency regulation capability in a solar photovoltaic power plant. *North American Power Symposium 2010, NAPS 2010*, pages 1–6, 2010. `doi:10.1109/NAPS.2010.5618965`.

[82] Walid A. Omran, M. Kazerani, and M. M. A. Salama. Investigation of Methods for Reduction of Power Fluctuations Generated From Large Grid-Connected Photovoltaic Systems. *IEEE Transactions on Energy Conversion*, 26(1):318–327, 2011. URL: `http://ieeexplore.ieee.org/document/5677463/`, `doi:10.1109/TEC.2010.2062515`.

[83] S. S. Choi, K. J. Tseng, D. M. Vilathgamuwa, and T. D. Nguyen. Energy storage systems in distributed generation schemes. *IEEE Power and Energy Society 2008 General Meeting: Conversion and Delivery of Electrical Energy in the 21st Century, PES*, pages 1–8, 2008. doi:10.1109/PES.2008.4596169.

[84] R. Bhatt and B. Chowdhury. *Grid Frequency and Voltage Support using PV Systems with Energy Storage.* URL: https://www. engineeringvillage.com/search/doc/abstract.url?{&}pageType= quickSearch{&}usageZone=resultslist{&}usageOrigin= searchresults{&}searchtype=Quick{&}SEARCHID= 1103616001a34de5b9660d75f5f6d0df{&}DOCINDEX=1{&}ignore{_}docid= inspec{_}10655dd133a330be6aM5c562061377553{&}da.

[85] N. Moreno-Alfonso J. M. Carrasco, L. G. Franquelo, J. T. Bialasiewicz, E. Galvan, R. C. Portillo-Guisado, M. A. M. Prats, J. I. Leon. Power-Electronic Systems for the Grid Integration of Renewable Energy Sources: A Survey. 53(102):1002–1016, 2004. arXiv: 1006.5277, doi:10.1109/TIE.2006.878356.

[86] Ha Thi Nguyen, Guangya Yang, Arne Hejde Nielsen, and Peter Hojgaard Jensen. Frequency stability improvement of low inertia systems using synchronous condensers. *2016 IEEE International Conference on Smart Grid Communications, SmartGridComm 2016*, pages 650–655, 2016. doi:10.1109/SmartGridComm.2016.7778835.

[87] Paul E. Marken, Arthur C. Depoian, John Skliutas, and Michael Verrier. Modern synchronous condenser performance considerations. *IEEE Power and Energy Society General Meeting*, pages 1–5, 2011. doi:10.1109/PES.2011.6039011.

[88] L. Wehenkel, T. H. Van Cutsem, and M. Ribbens-Pavella. An Artificial Intelligence Framework for On-Line Transient Stability Assessment of Power Systems, 1989. doi: 10.1109/MPER.1989.4310721.

[89] Kip Morison, Hamid Hamadanizadeh, and Lei Wang. Dynamic Security Assesment Tools. pages 282–286, 1999.

[90] T. E. Dy-Liacco. Enhancing power system security control. *IEEE Computer Applications in Power*, 10(3):38–41, 1997. doi:10.1109/67.595291.

[91] J N Fidalgo. Neural networks applied to preventive control measures for the dynamic security. 11(4):1811–1816, 1996.

[92] Dejan J Sobajic, Yoh-han Pao, Critical Clearing Time, Machine Learning Systems, Adaptive Pattern Recognition, and Rumelhart Neural-net. Artificial Neural-Net Based Dynamic Security. 4(1):220–228, 1989.

[93] A.B. Ranjit Kumar, A. Ipakchi, V. Brandwajn, M. El-Sharkawi, and G. Cauley. Neural networks for dynamic security assessment of large-scale power systems: requirements overview, 2002. doi:10.1109/ann.1991.213499.

[94] M. Djukanovic, D.J. Sobajic, and Y.-H. Pao. Neural net based determination of generator-shedding requirements in electric power systems. *IEE Proceedings C Generation, Transmission and Distribution*, 139(5):427, 2010. doi:10.1049/ip-c.1992.0060.

[95] SA Hatziargyriou, N Papathanassiou, JA Pecas-Lopes, and V Van Acker. *Pattern recognition versus decision trees methods-a case study in fast dynamic security assessment of autonomous power systems with a large penetration from renewables.* 1994.